Gallium solar neutrino experiments: Absorption cross sections, neutrino spectra, and predicted event rates

John N. Bahcall

School of Natural Sciences, Institute for Advanced Study, Princeton, New Jersey 08540
(Received 20 June 1997)

Neutrino absorption cross sections for ^{71}Ga are calculated for all solar neutrino sources with standard energy spectra, and for laboratory sources of ^{51}Cr and ^{37}Ar; the calculations include, where appropriate, the thermal energy of fusing solar ions and use improved nuclear and atomic data. The ratio, R, of measured (in GALLEX and SAGE) to calculated ^{51}Cr capture rate is $R = 0.95 \pm 0.07$ (expt)$+^{+0.04}_{-0.03}$ (theor). Cross sections are also calculated for specific neutrino energies chosen so that a spline fit determines accurately the event rates in a gallium detector even if new physics changes the energy spectrum of solar neutrinos. Theoretical uncertainties are estimated for cross sections at specific energies and for standard neutrino energy spectra. Standard energy spectra are also presented for pp and CNO neutrino sources in the appendix. Neutrino fluxes predicted by standard solar models, corrected for diffusion, have been in the range 120 SNU to 141 SNU since 1968. [S0556-2813(97)00912-6]

PACS number(s): 26.65.+t, 12.15.Ff, 14.60.Pq, 96.60.Jw

I. INTRODUCTION

Gallium solar neutrino experiments are, at present, the only detectors capable of detecting the fundamental pp neutrinos, which constitute about 90% of the neutrinos predicted by standard solar models to come from the Sun. The pioneering gallium solar neutrino experiments, GALLEX [1] and SAGE [2], are also unique in having been directly tested for efficiency of neutrino detection with a radioactive source, ^{51}Cr [3–6]. Moreover, the good agreement between the results of the two independent experiments, one of which uses gallium in chloride solution (GALLEX) and the other in a metallic form (SAGE), has led to increased confidence in the measured event rates. The results of the gallium experiments provide fundamental constraints on solar models and challenge the prediction of minimal electroweak theory that essentially nothing happens to neutrinos after they are created in the center of the Sun.

The Gallium Neutrino Observatory (GNO) Collaboration [7] has recently been formed to measure the solar neutrino event rate in a gallium detector over many years (at least one solar cycle) and with increased precision. The experiment, which may ultimately involve 100 tons of gallium, is designed to reduce both the systematic and the statistical errors so that an accuracy of about 5%, or 4 SNU, will be achieved if the final best-estimate event rate is 80 SNU.[1]

Motivated by the great importance of gallium solar neutrino experiments and the improvements possible with GNO, my goal in this paper is to calculate as accurately as possible the cross sections for absorption of solar neutrinos in a gallium detector and to explore more broadly the constraints on solar nuclear fusion provided by existing and future gallium experiments. The theoretical uncertainties in the capture cross sections, which are a function of neutrino energy, limit the ultimate interpretation of the observed results. Therefore, I devote a large part of the present paper to evaluating quantitatively the uncertainties that exist in the calculations of neutrino absorption cross sections.

I begin by summarizing in Sec. II the most important experimental data regarding the ^{71}Ga-^{71}Ge system. I describe in Sec. III how I evaluate the atomic effects of electron exchange and imperfect overlap between initial and final eigenstates, as well as the forbidden nuclear beta-decay corrections. I make use of new Dirac-Fock calculations of the electron density at the nucleus in a ^{71}Ge atom, in order to evaluate more accurately than was previously possible the f value for ^{71}Ge electron capture. In Sec. IV, I calculate the cross section for the absorption by ^{71}Ga of neutrinos from ^{51}Cr beta decay and compare the calculated value with the value inferred by the GALLEX and SAGE experiments and with the previous calculation. I describe in Sec. V the procedure I use to evaluate the uncertainties due to excited state transitions. I make conservative assumptions about the BGT (proportional to square of GT matrix elements) values that are determined by (p,n) reactions and follow Anselmann *et al.* [3] and Hata and Haxton [9] in using the results of the ^{51}Cr experiments performed by GALLEX and SAGE to constrain the neutrino absorption cross sections for transitions from the ground state of ^{71}Ga to the lowest two excited states of ^{71}Ge for which allowed captures are possible. I describe in Sec. VI the contributions to the energy spectra from the thermal energy of the fusing particles that produce neutrinos; these thermal energy contributions are included here for the first time in the calculation of the absorption cross sections.

If standard solar models and the minimal standard electroweak theory are correct, then the pp neutrinos provide the largest predicted contribution to gallium solar neutrino experiments. In Sec. VII, I evaluate the absorption cross section for pp neutrinos including for the first time the effect of the thermal energy of the fusing protons. I present in Sec. VIII

---

[1]A SNU is a convenient product of flux times cross section first defined in footnote 10 of Ref. [8], in 1969, to be 10^{-36} interactions per target atom per sec.

the results of calculations of the cross sections for the beta-decaying sources ^{8}B, ^{13}N, ^{15}O, and ^{17}F, emphasizing the uncertainties caused by transitions to excited states in ^{71}Ge. I present the cross section for the highest-energy solar neutrinos, the *hep* neutrinos, in Sec. IX.

The average cross section for the absorption of the ^{7}Be neutrino lines is important in understanding the implications of gallium solar neutrino measurements. I calculate in Sec. X the average cross sections for the ^{7}Be neutrino lines and for the *pep* line, including the thermal energy of the solar electrons and ions. I also calculate in Sec. X the cross section for absorption of neutrinos from a laboratory source of ^{37}Ar neutrinos.

Particle physics explanations of the solar neutrino measurements generally result in a modified neutrino energy spectrum for the electron-type neutrinos. Therefore, in Sec. XI, I present calculated best-estimate cross sections and 3σ different cross sections for a representative set of specific neutrino energies.

In Sec. XII, I calculate the event rate predicted by the current best standard solar model and compare the results with the rates measured by GALLEX and SAGE. I show in a figure the rates predicted by all standard solar models calculated by collaborators and myself since 1963. I also determine the rates predicted by solar models with crucial nuclear reactions artificially set equal to zero. I summarize and discuss the main results in Sec. XIII.

This paper also presents some additional data that are of general use in stellar evolution studies or for solar neutrino investigations. The average energy loss for each neutrino energy source, which is important for stellar evolution calculations, is given in the text that discusses the absorption cross section for that particular source. I tabulate in Appendix A the *pp* solar neutrino energy spectrum and in Appendix B the energy spectra for the CNO neutrino sources.

Unless stated otherwise, all nuclear data (including lifetimes, branching ratios, and mass differences, as well as their associated uncertainties), and also atomic binding energies, are taken from the 1996 8th edition of the *Table of Isotopes* [10].

II. GALLIUM-GERMANIUM DATA

I summarize in this section the basic data for the gallium-germanium system that are needed for the calculation of solar neutrino cross sections. I begin by listing in Sec. II A the best values and uncertainties for the most important measured atomic and nuclear quantities. Next, I calculate in Sec. II B the characteristic dimensional cross section factor σ_0 for gallium-germanium transitions. I conclude by discussing in Sec. II C what is known from (p,n) measurements about the matrix elements for transitions from the ground state of ^{71}Ga to different excited states of ^{71}Ge.

Figure 1 illustrates the most important neutrino transitions for a gallium solar neutrino experiment, provided that the incident neutrino flux is dominated, as expected on the basis of standard solar models, by neutrinos with energies less than 1 MeV.

A. Measured nuclear and atomic properties

The principal input data needed for the calculation of the neutrino cross sections are the atomic number $Z = 31$ and the
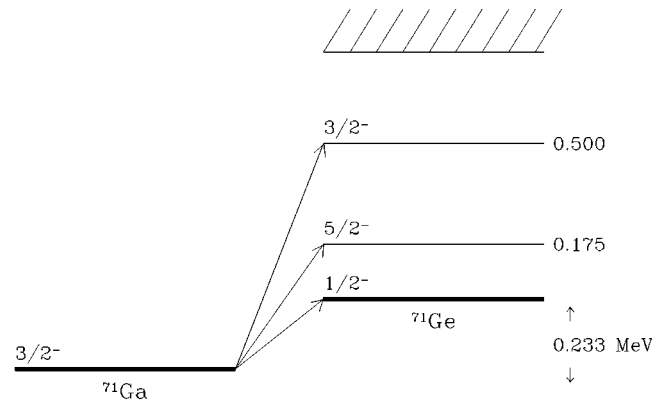

FIG. 1. The ^{71}Ga-^{71}Ge transitions for low energy neutrinos. Only the ground state and the first two allowed excited state transitions contribute to the absorption of pp, ^{7}Be, and ^{51}Cr neutrinos. The ^{8}B, CNO, and *pep* neutrinos all give rise to excited state transitions that are unconstrained by the ^{51}Cr neutrino absorption measurements and for which the (p,n) measurements provide the only empirical guide to the relevant BGT values.

atomic mass $A = 71$ of ^{71}Ga; the measured electron capture lifetime of ^{71}Ge, $\tau_{1/2}$; the neutrino energy threshold $E_{\text{threshold}}$; and the electronic binding energies in ^{71}Ga.

The lifetime for ^{71}Ge electron capture has been measured accurately by Hampel and Remsberg and is [11]

$$\tau_{1/2} = (11.43 \pm 0.03)d. \qquad (1)$$

The energy threshold has been measured in a number of different experiments. The value of $E_{\text{threshold}} = 233.2 \pm 0.5$ keV due to Hampel and Schlotz [12] was used in the previous calculations [13,14] of gallium absorption cross sections. There have subsequently been three additional measurements in the context of the search for a possible 17 keV neutrino; they are 229.1 ± 0.6 keV [15], 232.1 ± 0.1 keV [16], and $232.65^{+0.17}_{-0.12}$ [17]. The result from the first of these three measurements is somewhat uncertain since these authors [15] found evidence for a 17 keV neutrino in their internal bremsstrahlung spectrum. A weighted average of all the available measurements, including estimates of systematic errors, has been computed by Audi and Wapstra [18], who find

$$E_{\text{threshold}} = 232.69 \pm 0.15 \text{ keV}. \qquad (2)$$

The s-shell binding energies of the K, L, and M electrons in ^{71}Ga, which are needed below for the calculation of σ_0, are, respectively, 10.37 keV, 1.30 keV, and 0.16 keV.

B. Calculation of σ_0

Neutrino absorption cross sections from the ground state of ^{71}Ga to the ground state of ^{71}Ge are inversely proportional to the ft value for the inverse process, the electron capture decay of ^{71}Ge to ^{71}Ga. The precise form of this relation is given in Eq. (11) of Ref. [19], which defines a characteristic neutrino absorption cross section σ_0 in terms of the electron capture rate from the ground state of the daughter nucleus produced by neutrino capture. The quantity σ_0 is used as an overall scale factor in detailed numerical calculations of neutrino absorption cross sections.

Inserting the best available estimates for the electron capture lifetime, Eq. (1), and energy threshold, Eq. (2), in Eq. (11) of Ref. [19] yields

$$\sigma_0 = \frac{1.2429 \times 10^{-47} \text{cm}^2}{\Sigma_i q_i^2 g_i^2}, \tag{3}$$

where $q_i = E_{\text{threshold}} - E_{\text{binding},i}$ and g_i^2 is the square of the radial electron wave function, averaged over the nuclear volume, for the ith atomic state in ^{71}Ge . The numerical coefficient in Eq. (3) is appropriate when q_i is measured in $m_e c^2$ and g_i^2 is measured in $(\hbar/m_e c)^{-3}$.

I have recalculated σ_0 using the results of a special series of evaluations of the ^{71}Ge electron wave functions generously performed for application to this work by I. Grant [20], W. Johnson et al. [21], and M. Chen [22]. All three of the calculations use relativistic, self-consistent Dirac-Fock codes that include the effects of finite-sized nuclei, the Breit interaction, vacuum polarization, and self-energy corrections. Details of the codes used are supplied in the references just cited. I have averaged the values of g_i^2 over the nuclear volume using data supplied by Grant, Johnson, and Chen. The total spread among the three calculations is only $\pm 0.2\%$, which does not contribute significantly to the overall error budget of the cross section calculations.

Using the new relativistic Hartree Fock calculations [20–22] and the slightly improved energy threshold given in Eq. (2), I find

$$\sigma_o = 8.611 \times 10^{-46} \ \text{cm}^2, \tag{4}$$

with an overall (effective 3σ) systematic uncertainty of 0.4% that is common to all cross sections quoted in this paper and which should be treated as an additional theoretical uncertainty (not included elsewhere) in precise error analyses of gallium solar neutrino experiments. The value of σ_0 given in Eq. (4) is about 0.5% less than the value of $\sigma_0 = 8.8012 \times 10^{-46}$ cm^2 that I have used since 1984 (see Refs. [13,14,23]). All the published calculations on the implications of gallium solar neutrino experiments with which I am familiar have also made use of this previous determination of σ_0.

The short-distance high-momentum loop radiative corrections are automatically taken into account by scaling all of the neutrino capture cross sections relative to the electron capture rate that determines σ_0 [24,25]. The additional radiative corrections are expected to be smaller than the short distance corrections and therefore significantly less than other uncertainties estimated in this paper [25].

C. Transitions to excited states

The most important uncertainties in the calculation of absorption cross sections for solar neutrinos incident on ^{71}Ga are related, for all but the lowest-energy neutrinos, to the transition matrix elements to excited states in ^{71}Ge (see, e.g., Refs. [13,19,9]). In what follows, I shall make use of the BGT values for transitions to excited states of ^{71}Ge that are estimated by studying (p,n) reactions. The BGT values determined by Krofcheck and his colleagues [23,26] are listed in Table I. In order to help make clear which transitions are

TABLE I. Gamow-Teller strength functions in ^{71}Ge as measured by (p,n) reactions [23,26].

E_{ex} (MeV)	BGT/(BGT)$_{\text{g.s.}}$
0.0	1.000
0.175	<0.056
0.50	0.146
0.80	0.451
1.25	0.404
1.75	0.485
2.25	0.443
2.75	1.101
3.25	1.680
3.75	2.746
4.25	3.300
4.75	3.380
5.25	3.265
5.75	5.387
6.25	5.944
6.75	4.924
7.20	1.573

most important, I have presented the estimated BGT values relative to the BGT value of the ground-state to ground-state transition. The resolution obtained in the experiments of Krofcheck et al. is about 300 keV; this resolution is not always sufficient to identify the particular final state(s) in ^{71}Ge to which the strength of the (p,n) reaction refers (cf. the discussion of the cross section for the pep line in Sec. X B). The transition to the $5/2^-$ first excited state of ^{71}Ge at an excitation energy of 175 keV was too weak to be measured and only an upper limit was determined. In the discussion that follows, I shall use for definiteness a BGT value that is one-half of the measured upper limit, i.e., BGT(175 keV)/(BGT)$_{\text{g.s.}}$ = 0.028.

I follow Anselmann et al. [3] and Hata and Haxton [9] in using the GALLEX [3–5] and SAGE [6] measurements of ^{51}Cr neutrino absorption by ^{71}Ga to constrain the BGT values for solar neutrino detection (see Sec. IV E).

III. OVERLAP, EXCHANGE, AND FORBIDDEN EFFECTS

I summarize in this section how I calculate atomic overlap and exchange effects and nuclear forbidden effects.

A. Overlap and exchange effects

The change in nuclear charge by one unit in beta decay and in neutrino capture causes the initial and final atomic eigenstates to overlap imperfectly, which is known as the "overlap" effect in atomic beta decay. Antisymmetrization between bound and continuum electrons, the "exchange effect," has a measurable effect in determining electron capture ratios and decreases the calculated cross sections for neutrino capture reactions by a small, calculable factor.

Overlap and exchange effects were first discussed in detail in Ref. [27] and applied in Ref. [19] to the calculation of neutrino capture cross sections. Experiments on electron capture ratios provide strong evidence for the validity of the

electron exchange corrections (see Ref. [28] for an early discussion). I use Eq. (13) and Eq. (14) of Ref. [19] to evaluate numerically the atomic overlap and exchange effects. In previous calculations, I have been content with showing that these corrections are small, less than or of order 1% [19], and have not included them explicitly in the numerical calculations.

The imperfect overlap between initial and final atomic states adds 0.09 keV to the usually tabulated mass difference between neutral atoms for the case of neutrino capture by gallium; this small energy difference, which slightly increases the threshold energy, is not included in Eq. (2), but is taken account of in the numerical calculations described in the present paper.

The overlap effect is not significant for our purposes. Even for the low-energy pp neutrinos, the overlap effect decreases the calculated absorption cross section by less than 0.1%.

Exchange effects between the final continuum electron and the electrons bound in the initial atom interfere in a way that reduces slightly the calculated capture rate [27,19]. In the calculations described later in this paper, I evaluate the exchange effect for gallium cross sections by using Eq. (14) of Ref. [19]. For the pp cross section which is evaluated in Sec. VII, exchange effects reduce the calculated cross section by 0.4%. In all other cases, the calculated effects of electron exchange are negligible, because the characteristic energies of solar neutrinos (MeV) are much larger than the characteristic binding energies of the atomic electrons (keV).

B. Forbidden corrections

Forbidden corrections to nuclear beta decay have been calculated by many workers. I follow here the prescription due to Holstein and Treiman [29], which has been applied by Bahcall and Holstein [30] to solar neutrino problems. I use for the best-estimate calculations presented in the present paper the approximations that are described in the Appendix of Ref. [30].

Since the forbidden corrections involve estimates of unmeasurable nuclear matrix elements, I regard the calculated corrections as only an indication of the likely size of forbidden effects. With the Bahcall-Holstein approximations, the forbidden effects vary slowly between 2% and 2.5% at neutrino energies less than about 10 MeV and then change sign, becoming approximately zero at 15 MeV. This cancellation near 15 MeV is presumably an artifact of the choice by Bahcall and Holstein of characteristic nuclear parameters that were intended to apply approximately over a wide range of nuclei. In the energy regime relevant to supernovae neutrinos but just beyond the reach of nearly all solar neutrinos, 15–30 MeV, the calculated forbidden corrections rise rapidly, approximately proportional to the square of the recoil electron energy.

For the purpose of estimating uncertainties, I adopt the conservative approach of replacing the decrease in the calculated forbidden corrections in the region 10–15 MeV by a monotonic estimate of $0.025(q/10 \text{ MeV})^2$ for neutrino energies above 10 MeV. This procedure ignores the cancellation that occurs near 15 MeV, but otherwise gives a relatively accurate numerical representation of the higher-energy for-
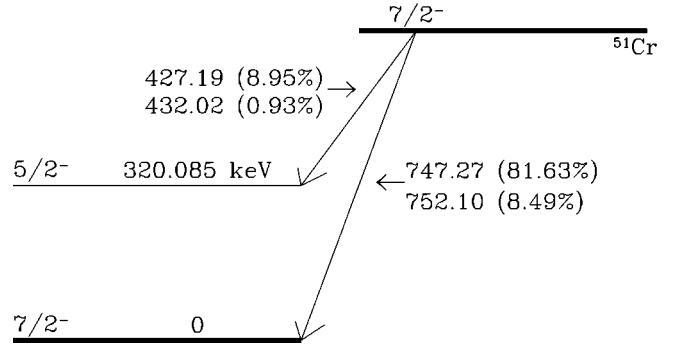
^{51}Cr Neutrino Decay

FIG. 2. The ^{51}Cr decay scheme.

bidden corrections as described in Ref. [30].

I adopt three times the best-estimate forbidden correction as a 3σ uncertainty due to forbidden corrections. I ignore the calculated sign of the forbidden corrections and instead assume that both the estimated minimum and the estimated maximum cross sections have a contribution from forbidden terms of equal magnitude (added quadratically with other uncertainties).

Fortunately, for solar neutrino cross sections, the forbidden corrections are never fractionally very large. For all cases except for the pp neutrinos, the uncertainties due to transitions to excited states are much larger than the uncertainties due to forbidden corrections. However the uncertainties become very large, about a factor of 3, above 25 MeV (see Sec. XI).

IV. CHROMIUM NEUTRINO ABSORPTION CROSS SECTION

The overall efficiency for the detection of neutrinos with radiochemical gallium detectors has been measured directly in two historic experiments by the GALLEX [3–5] and the SAGE [6] solar neutrino collaborations using intense ^{51}Cr sources of low-energy neutrinos. Originally proposed by Kuzmin [31] and Raghavan [32], these calibration experiments show that the neutrino detectors work as expected. The ^{51}Cr neutrino sources are especially useful for testing the detection efficiency since the chromium neutrinos are similar in energies to the pp and ^{7}Be solar neutrinos to which the gallium detectors are most sensitive. In addition to being the first direct tests of solar neutrino experiments with an artificial source of neutrinos, the calibration results also improve by more than an order of magnitude previous limits on Δm^2 for electron-neutrino oscillation experiments at accelerators [33]. Moreover, Anselmann et al. [3] and Hata and Haxton [9] have shown that the test results provide useful direct constraints on the BGT values for excited state transitions from the ground state of ^{71}Ga to excited states of ^{71}Ge that must otherwise be inferred from the less-easily interpreted (p,n) experiments (cf. Sec. II).

Figure 2 shows the four neutrino lines that are produced by the decay of ^{51}Cr [10].

A. Experimental results

The experimental results on ^{51}Cr neutrino absorption are reported [3,4,6] as a ratio R of the measured cross section to the value of the cross section calculated by Bahcall and Ulrich in 1988 [13]. Thus

$$R \equiv \frac{\sigma(^{51}\text{Cr})_{\text{measured}}}{\sigma(^{51}\text{Cr})_{\text{BU88}}}. \qquad (5)$$

The value of the previous standard cross section is [13]

$$\sigma(^{51}\text{Cr})_{\text{BU88}} = 59.2 \times 10^{-46}(1 \pm 0.1) \text{ cm}^{-2}, \quad 3\sigma, \quad (6)$$

where the total theoretical error quoted in Eq. (6) is an effective 3σ uncertainty.

The measured values, with their quoted 1σ errors, are [3,4]

$$R(\text{GALLEX}) = 0.92 \pm 0.08, \quad 1\sigma \qquad (7)$$

and [6]

$$R(\text{SAGE}) = 0.95 \pm 0.12, \quad 1\sigma. \qquad (8)$$

The weighted average value for R, $\langle R \rangle$, obtained by combining the results from the two experiments, is very similar to the GALLEX value. One finds

$$\langle R \rangle = 0.93 \pm 0.07, \quad 1\sigma. \qquad (9)$$

The errors quoted in Eqs. (7)–(9) for the experimental results do not include the uncertainty in the theoretical calculation that is given in Eq. (6).

B. Measured quantities characterizing chromium decay

The Q value or atomic mass difference between the ground states of ^{51}Cr and ^{51}V is

$$Q = 752.73 \pm 0.24 \text{ keV}. \qquad (10)$$

A preliminary result from the remeasurement of the Q value using internal bremsstrahlung from the ^{51}Cr decay carried out by Hampel [34] gives a result in good agreement with Eq. (10).

As shown in Fig. 2, electron capture by ^{51}Cr leads to the ground state of ^{51}V with a branching ratio of 90.12% and to the first excited state with a branching ratio of 9.88%. The neutrino energy released in the electron capture reaction leading to the ^{51}Cr ground state is $Q - E(K) = 747.27$ keV, where $E(K) = 5.46$ keV is the binding energy of the K electron in ^{51}V. The neutrino energy corresponding to L capture is $Q = 752.73 - 0.63$ keV or 752.10 keV. The neutrino energies that result from K and L captures to the first excited state of ^{51}V are 432.02 keV and 427.19 keV, respectively. The measured capture ratio is [35]

$$L/K = 0.104 \pm 0.003, \quad 1\sigma. \qquad (11)$$

C. Best estimate

The best-estimate neutrino absorption cross section averaged over the four neutrino lines of ^{51}Cr is

$$\sigma(^{51}\text{Cr})_{\text{best}} = 58.1(1^{+0.036}_{-0.028}) \times 10^{-46} \text{ cm}^2, \quad 1\sigma. \qquad (12)$$

In computing the cross section given in Eq. (12), I have used the Q value for the chromium decay given in Eq. (10), the gallium threshold given in Eq. (2), and the characteristic gallium cross section σ_0 given in Eq. (4). The current best the-

oretical estimate for the average cross section for ^{51}Cr neutrinos given in Eq. (12) is 2% smaller than the previous value [cf. Eq. (6)]. The value computed here is 5.4% larger (less than 1σ larger) than the best-estimate experimental value of 55.1×10^{-46} cm^2 [cf. Eq. (9)].

Most of the computed cross section comes from transitions between the ground state of ^{71}Ga and the ground state of ^{71}Ge. The fraction of the total cross section that arises from ground-state to ground-state transitions is

$$\sigma(^{51}\text{Cr})_{\text{g.s.}}/\sigma(^{51}\text{Cr})_{\text{best}} = 0.95. \qquad (13)$$

D. Uncertainties

The largest uncertainty in the prediction of the ^{51}Cr absorption cross section arises from the poorly known matrix elements for the transitions from the ground state of ^{71}Ga to the excited states of ^{71}Ge [13,19,9]. I have used as best estimates for excited state transitions the BGT values that were determined from (p,n) measurements by Krofcheck and his associates [23,26] (see Table I). I have taken the minimum contribution from excited states to be zero and regard this decrease, -4.8%, from the best-estimate value as a 3σ change.

For the maximum 3σ contribution from excited states, I have multiplied the BGT values determined by (p,n) measurements by a factor of 2. More explicitly, I multiplied the measured (p,n) upper limit BGT value to the first excited state, BGT/BGT$_{\text{g.s.}} < 0.056$, by a factor of 2 and the measured value to the second excited state, BGT/BGT$_{\text{g.s.}} = 0.146$, also by a factor of 2. In all ten cases in which (p,n)-inferred BGT values for weak transitions have been compared to accurately measured beta-decay matrix elements, the (p,n) values are about equal to or much larger than the true beta-decay matrix elements. It is possible [9] that this consistent trend is due to a special selection rule operating in all ten of the cases in which both the beta-decay and (p,n) measurements have been made accurately. However, there is additional information available to support the procedure adopted here. The two cases which are most relevant to the current discussion occur in the decay of ^{37}Ca to ^{37}K; these are the only two cases with which I am familiar in which the corresponding beta decay matrix elements are very small, comparable to the BGT values determined by the (p,n) measurements for the weak transitions to the first two excited states of ^{71}Ge. For these two weak transitions, the measured BGT values from beta-decay are between one and two orders of magnitude smaller than the BGT values inferred from (p,n) measurements [9]. Therefore, the upper limit change, $+8.4\%$, determined by multiplying the (p,n)-inferred BGT value, and the upper limit BGT value to the lowest excited state, both by a factor of 2 seems like a reasonable effective 3σ upper limit to the contribution of excited state transitions to the best-estimate value.

The next largest uncertainty is from forbidden corrections to the beta-decay matrix elements [30]. Omitting entirely the forbidden corrections decreases the calculated cross section by 2.3%. I regard this decrease as a 1σ uncertainty, which in principle could either decrease or increase the cross section, since the magnitude of the forbidden correction is only an estimate [30].

The uncertainty in the ^{51}Cr Q value causes an uncertainty of $\pm 0.05\%$, the ^{71}Ga threshold $\pm 0.2\%$, and the ^{71}Ga lifetime $\pm 0.3\%$.

Combining all of the uncertainties described above, I find an effective 1σ uncertainty of $+3.6\%$ (-2.8%) in the theoretical prediction of the cross section for absorption of ^{51}Cr neutrinos by ^{71}Ga. Three times the 1σ uncertainties quoted here are comparable to the previously estimated [13] effective 3σ uncertainty of $\pm 10\%$. The excellent agreement with the measured value GALLEX and SAGE values [3,4,6] is not significantly affected by the recalculation described in this subsection.

The 3σ lower limit from excited state contributions that is adopted here, namely, the zero contribution, is absolutely reliable. There is no way of giving a similarly reliable *theoretical* upper limit for the contribution of excited states. In fact, Hata and Haxton have argued that the only convincing upper limit is determined by the ^{51}Cr measurements themselves.

E. Constraint on excited state transitions

Anselmann *et al.* [3] and Hata and Haxton [9] have shown how the measurements by GALLEX and SAGE of the capture rate by ^{51}Cr neutrinos can be used as a constraint on the strength of the absorption transitions leading to the $5/2^-$ state at 175 keV and the $3/2^-$ state at 500 keV. The measured capture rate, given in Eq. (5), Eq. (6), and Eq. (9), can be written as the ratio of the contributions to the ground state, the first excited state at 175 keV, and the excited state at 500 keV, all divided by the ground-state to ground-state cross section. The ratio of the previously standard cross section, Eq. (6), to the best current value for the ground-state to ground-state transition, $\sigma(^{51}\text{Cr})_{\text{g.s.}} = 55.3 \times 10^{-46}$ cm^2, is 1.071. With a little algebra, one finds

$$\left[0.669 \frac{\text{BGT(175 keV)}}{\text{BGT}_{\text{g.s.}}} + 0.220 \frac{\text{BGT(500 keV)}}{\text{BGT}_{\text{g.s.}}} \right]$$
$$= -0.004 \pm 0.075, \qquad (14)$$

where the ratio of the cross sections $\sigma(175 \text{ keV})/\sigma_{\text{g.s.}}$ would be 0.669 if the BGT values for the two transitions were equal [and $\sigma(175 \text{ keV})/\sigma_{\text{g.s.}}$ would be 0.220 if the BGT values were equal]. Equation (14) implicitly assumes that the detection efficiency for the gallium experiments is close to unity; this assumption is based upon independent tests for the detection efficiency that are described in the original experimental papers [1,2].

The coefficients in Eq. (14) are slightly different from those given by Hata and Haxton, reflecting the slightly improved data described in Sec. II. In what follows, I shall use the prescription of the Particle Data Group [36] for estimating confidence limits; namely, I shall assume that the errors shown in Eq. (14) are normally distributed with a mean value at -0.004 but with a renormalized probability distribution that is nonzero only when the manifestly positive quantity between the brackets in Eq. (14) is positive.

At the 3σ limit, Eq. (14) allows maximum values of BGT$(175 \text{ keV})_{3\sigma} = 12 \times$ BGT$(175 \text{ keV})_{p,n}$ and BGT$(500 \text{ keV})_{3\sigma} = 6.8 \times$ BGT$(500 \text{ keV})_{p,n}$ where the values of BGT$_{p,n}$ are described in Sec. II C. These maximum values of

12 and 7 times the indicated (p,n) BGT values are consistent with the constraints suggested by Hata and Haxton. These 3σ upper limits are probably unrealistically conservative since the available evidence shows that (p,n) reactions overestimate the strength of two very weak beta-decay transitions (see Sec. IV D and Ref. [9]). I have also implemented the 3σ limits in a conservative way: I use the upper limit value for BGT(500 keV) [with BGT(175 keV)=0] whenever the 500 keV state is above threshold, since the ^{51}Cr limit allows a somewhat larger BGT value for a 500 keV excited state than for a 175 keV excited state. I use the upper limit value for BGT(175 keV) below threshold of the 500 keV state. This simplistic prescription causes a slight discontinuity in the upper error estimate near 500 keV.

V. UNCERTAINTIES DUE TO EXCITED STATE TRANSITIONS

I calculate the allowed 3σ lower limit for all neutrino sources except the high-energy ^{8}B and *hep* neutrinos by setting equal to zero the matrix elements for all excited state transitions. For the 3σ upper limit to the weak transitions to the first two allowed excited states (Fig. 2), I follow Hata and Haxton [9] and use the constraint provided by the ^{51}Cr measurements that is given in Eq. (14). As discussed in Sec. IV E, this ^{51}Cr constraint allows one of the transitions to be an order of magnitude larger than indicated by the (p,n) measurements; a difference this large has not been observed in any case in which accurate beta-decay measurements could be compared with the results of (p,n) experiments [9]. Indeed, for intrinsically weak transitions like the ones we are discussing, the (p,n) experiments overestimate by an order of magnitude the BGT values in the two cases for which a comparison has been possible.

For higher-energy neutrinos that can excite the many other GT transitions, I determine as before the 3σ lower limit by dividing by two the BGT values determined by (p,n) experiments and the 3σ upper limit by multiplying the (p,n) BGT values by a factor of 2. This is also an extreme range since for moderately strong transitions a good correlation exists between the forward-angle (p,n) cross sections and the measured β-decay strength [37].

The limits given later in this paper represent maximal changes in that I assume that all of the excited states are increased together, or decreased together, to their extremal values. I combine linearly (rather than quadratically) the uncertainties from different excited states.

VI. SOLAR THERMAL EFFECTS

The neutrino energies for laboratory weak interactions are shifted by small amounts, ΔE, due to the thermal energy of the particles that produce the neutrino emission. In general, one can write

$$q_\odot = q_{\text{lab}} + \Delta E, \qquad (15)$$

where q_{lab} and $q_\odot$ are, respectively, the neutrino energies emitted in laboratory experiments and in the solar interior. The energy shifts are negligible for isolated nuclei, like ^{8}B, ^{13}N, ^{15}O, and ^{17}F, that beta decay in the Sun [38]. The physical reason for the smallness of the thermal effects in

these cases is that the initial decaying state contains only a single nucleus, unlike the situation in the pp reaction in which two fusing protons use their initial kinetic energetic to penetrate the Coulomb barrier between them. The random nature of the thermal velocities causes all first order effects in the velocities of the ions to vanish. Therefore the change in shape is of order the temperature divided by the typical neutrino energy or keV over MeV.

However, when two or more particles are involved in neutrino production, e.g., the pp reaction or ^{7}Be electron capture, the thermal shifts can produce small changes in the neutrino energies and therefore neutrino absorption cross sections. These shifts due to the addition of the stellar thermal energy to the laboratory decay energy are close to the level of current experimental sensitivity.

The energy shifts ΔE have previously been included in the energy balance [13], at least in the nuclear energy generation code that I have written and made publicly available [39]. However, the extra thermal energy has not been previously included in the calculated absorption cross sections. I summarize in this section the expected thermal energy shifts that will be used in the following sections. The energy shifts have been calculated in Refs. [13,38,40].

The most important thermal contributions to the neutrino energy spectrum are for the abundant, low-energy pp neutrinos. An explicit calculation for the average center-of-mass energy contributed by the two fusing protons yields [38], Eq. (52),

$$\Delta E(pp) = 3.6 \times \langle d\phi_{pp}(T)(T/15 \times 10^6 \text{ K})^{2/3}\rangle \text{ keV,} \tag{16}$$

where T is the ambient temperature. The average indicated in Eq. (16) by the angular brackets is taken over the temperature profile of the Sun weighted by the fraction of the pp flux, $d\phi_{pp}(T)$, that is produced at each temperature. This average is insensitive to the details of the solar model.

I have calculated the average for four different solar models: the 1992 Bahcall-Pinsonneault models [41] with and without helium diffusion and the 1995 Bahcall-Pinsonneault models [42] with and without helium and heavy element diffusion. The results for the four models can be summarized as follows:

$$\langle d\phi_{pp}(T)(T/15 \times 10^6 \text{ K})^{2/3}\rangle = 0.882 \pm 0.004, \tag{17}$$

where the error shown is an indication of the systematic uncertainty. Thus the thermal energy shift for the pp neutrinos is

$$\Delta E(pp) = 3.18 \pm 0.02 \text{ keV.} \tag{18}$$

The variations in the energy shift from one solar model to another that are indicated in Eq. (17) are only about 20 eV, which is less than 0.01% of the total pp energy.

For the much higher energy hep neutrinos, the thermal energy shift is [38], Eq. (53),

$$\Delta E(hep) = 5.4 \times \langle d\phi_{hep}(T)(T/15 \times 10^6 \text{ K})^{2/3}\rangle \text{ keV.} \tag{19}$$

Using the same four solar models cited above in connection with the evaluation of the weighted average pp energy shift, I find for the hep thermal energy shift

$$\Delta E(hep) = 4.76 \pm 0.02 \text{ keV.} \tag{20}$$

The 20 eV model dependence of the hep energy shift is negligible compared to the 18.8 MeV endpoint energy.

I have performed elsewhere [40] a detailed calculation of the shape of the energy profile of neutrinos produced by ^{7}Be electron capture in the Sun. The average energy for a neutrino emitted in the Sun can be expressed as the sum of the energy for a laboratory decay plus a small correction due to the solar thermal energy. I find [40]

$$\langle q_\odot(^7\text{Be})\rangle = 861.8 \text{ keV} + 1.28 \text{ keV} = 863.1 \text{ keV,} \quad 89.7\%, \tag{21}$$

$$\langle q_\odot(^7\text{Be})\rangle = 384.3 \text{ keV} + 1.24 \text{ keV} = 385.5 \text{ keV,} \quad 10.3\%. \tag{22}$$

When the energy shifts were evaluated using different solar models, the spread in energy shifts was found to be less than 10 eV [40].

The energy shift for the pep neutrinos has not yet been calculated accurately, but this does not cause any significant uncertainty in the predicted solar event rates since [14] the calculated pp flux is about 400 times larger than the pep flux and the ^{7}Be flux is about 40 times larger.

VII. pp NEUTRINO ABSORPTION CROSS SECTION

In standard model calculations, the largest predicted contribution to the event rate of gallium solar neutrino experiments is from the flux of pp solar neutrinos [14]. In this section, I reevaluate the neutrino absorption cross section for pp neutrinos including for the first time the effect of the thermal energy of the fusing protons and making use of the ^{51}Cr constraint described in Sec. IV. I include overlap and exchange effects according to the prescription derived in Refs. [27,19]. Exchange and overlap effects reduce the calculated pp cross section by about 0.4% and by less than 0.1%, respectively.

Appendix A contains a numerical representation of the pp neutrino energy spectrum that should be sufficient for most particle physics applications. In the calculations reported on here, I have used a more detailed pp spectrum, available elsewhere [39], that contains the relative intensity at 8000 different energies.

The q value for the pp reaction can be computed from the accurately known and tabulated [10] masses of the neutral atoms and is

$$q_{\text{lab}} = 420.220 \pm 0.022 \text{ keV.} \tag{23}$$

Since hydrogen is ionized in the Sun, the mass difference for neutral atoms should be increased, for solar calculations, by the binding energy of a K electron, 0.014 keV. Adding the thermal energy contributed by the fusing protons [see Eq. (18) or Ref. [38]] and the K-shell binding energy, one finds, for the end point energy of the solar pp energy spectrum,

$$q_\odot = 423.41 \pm 0.03 \text{ keV.} \tag{24}$$

The average energy loss from a star per emitted neutrino for an unmodified pp energy spectrum is an important datum for stellar evolution calculations and is

$$\langle q_\odot \rangle = 266.8 \text{ keV}. \tag{25}$$

The best-estimate ^{71}Ga absorption cross section for pp-electron-type neutrinos with a standard model energy spectrum incident is

$$\sigma(pp) = 11.72[1.0 \pm 0.023] \times 10^{-46} \text{ cm}^2, \quad 1\sigma. \tag{26}$$

Nearly all of the pp cross section arises from ground-state to ground-state transitions. Only 0.05% of the calculated cross section given in Eq. (26) is estimated to arise from transitions to the first excited state of ^{71}Ge.

The value of the pp cross section given in Eq. (26) is, as a result of a number of canceling changes, only 0.7% less than the previously calculated value [13,14]. Adding the solar thermal energy to the laboratory q value increases the cross section by about 1.6%. The more precise evaluation of σ_0 (cf. Sec. II B), due primarily to improved calculations of the electron wave functions and a more precise energy threshold, decreases σ_0 by about 2.2% . The smaller threshold increases the calculated phase space, and exchange effects reduce the capture cross section, both by about 0.4%. Other corrections result in smaller changes.

The largest 1σ uncertainties in calculation of the pp cross section are caused by forbidden corrections ($\pm 2.3\%$), the matrix element from the ground state of ^{71}Ga to the first excited state of ^{71}Ge ($+0.19\%$, -0.02%), the lifetime of ^{71}Ge ($\pm 0.26\%$), and the ^{71}Ga-^{71}Ge neutrino energy threshold ($\pm 0.1\%$). I have taken the $\pm 1\sigma$ uncertainty due to forbidden corrections to be equal to the decrease in the calculated cross section when forbidden terms are set equal to zero. The 3σ lower limit due to excited states was evaluated by setting equal to zero the matrix element for the only excited state transition that is energetically allowed. The upper limit was determined by evaluating the maximum allowed excited state contribution that is consistent with the constraint imposed by the ^{51}Cr measurements [see Eq. (14)].

VIII. ^{8}B, hep, ^{13}N, ^{15}O, AND ^{17}F NEUTRINOS

The calculation of the absorption cross sections for neutrinos from the beta-decaying sources, ^{8}B, ^{13}N, ^{15}O, and ^{17}F, is simpler than for the pp neutrinos because the shapes of the neutrino energy spectra are changed by at most one part in 10^5 by solar effects [38].

The effects of excited state transitions are significant for all of the neutrino sources considered in this section, again unlike the pp reaction in which the neutrino energy is too low for there to be a significant probability for exciting the final nucleus.

A. ^{8}B neutrinos

For the ^{8}B neutrinos, I use the recently determined best-estimate neutrino spectrum [43] and the improved gallium input data (see Sec. II) to obtain a best-estimate absorption cross section of

$$\sigma(^8\text{B}) = 2.40[1.0^{+0.32}_{-0.15}] \times 10^{-42} \text{ cm}^2, \quad 1\sigma. \tag{27}$$

The value given in Eq. (27) is essentially identical to the cross section calculated in Ref. [43]. However, the system-atic uncertainties in this cross section are large, because there has not been any significant improvement in our understanding of the relation between (p,n) reactions and Gamow-Teller transition strengths.

The principal uncertainty in estimating the cross section for ^{8}B neutrinos is caused by the dominant contribution of excited states to the total cross section. For ^{8}B neutrinos, the ground-state to ground-state transition accounts for only 12% of the best-estimate total cross section. Since transitions to many different excited states contribute to the ^{8}B absorption cross section, it is reasonable to assume that the stronger transitions dominate. In estimating the uncertainties from excited state transitions, I have taken advantage of the fact that for relatively strong GT transitions the measured (p,n) cross sections give BGT values that agree reasonably well with BGT values determined directly from beta decay [9]. I have therefore followed my usual practice [14] and estimated the 3σ upper uncertainties for excited state transitions by doubling the contribution estimated from (p,n) reactions and the 3σ lower uncertainty by halving the calculated contribution from excited states. The uncertainties due to the shape of the ^{8}B neutrino energy spectrum and to forbidden corrections (see Ref. [43]) are much smaller, only 1.5% and 2.4%, respectively.

The neutrino energy spectrum from ^{8}B beta decay does not have a sharp cutoff because the predominantly populated final state in ^{8}B is broad. The average neutrino energy emitted is

$$\langle q_\odot \rangle = 6.735 \text{ MeV} \pm 0.036 \text{ MeV}, \tag{28}$$

where the error estimate represents a 1σ uncertainty, as defined in Ref. [43], in the standard neutrino energy spectrum.

B. CNO neutrinos

I recalculate the cross sections for CNO neutrinos in this subsection. The changes from previous best-estimate values [13] are small in all cases. The estimated uncertainties given here are larger than I previously estimated because I now use extreme criteria for determining the allowed range of contributions from excited state transitions (see Sec. V).

In Appendix B, I present the calculated spectral energy distributions for the three CNO neutrino sources. These standard energy distributions are useful for many particle physics applications, but I have not previously published the CNO neutrino energy spectra.

The best-estimate absorption cross section for ^{13}N neutrinos is

$$\sigma(^{13}\text{N}) = 60.4[1.0^{+0.06}_{-0.03}] \times 10^{-46} \text{ cm}^2, \quad 1\sigma. \tag{29}$$

The cross section given here corresponds to a spectrum with a maximum neutrino energy of

$$q_\odot = 1.1982 \pm 0.0003 \text{ MeV}, \tag{30}$$

which is about 1 keV smaller than I have used previously. I have taken account in the present calculation of the difference in binding energies between initial and final neutral atomic states in the laboratory. The average energy loss accompanying ^{13}N beta decay is

$$\langle q_\odot \rangle = 706.3 \text{ keV}. \tag{31}$$

The upper-limit uncertainty is dominated by our lack of knowledge of the transition rates to excited states. The 3σ upper limit is chosen so as to yield the maximum possible cross section for ^{13}N neutrinos consistent with the constraint, Eq. (14), from the ^{51}Cr experiment. The uncertainty from forbidden corrections is added quadratically, but is relatively small. The 3σ lower limit is determined by setting to zero the cross sections for all excited state transitions and by multiplying by 3 the change in the cross section that results from ignoring all forbidden corrections. The effects of dropping excited state transitions and of ignoring forbidden corrections have been added quadratically.

The best-estimate absorption cross section for ^{15}O neutrinos is

$$\sigma(^{15}\text{O}) = 113.7[1.0^{+0.12}_{-0.05}] \times 10^{-46} \text{ cm}^2, \quad 1\sigma. \tag{32}$$

The maximum neutrino energy of the ^{15}O neutrino energy spectrum is

$$q_\odot = 1.7317 \pm 0.0005 \text{ MeV}, \tag{33}$$

after taking account of the difference in binding energies between initial and final neutral atomic states in the laboratory. The upper-limit and lower-limit uncertainties are determined as described above for ^{13}N neutrinos. The average energy loss accompanying ^{15}O beta decay is

$$\langle q_\odot \rangle = 996.4 \text{ keV}. \tag{34}$$

The cross section calculations for ^{17}F neutrinos are almost identical to those for ^{15}O since the end point energies are almost the same. I find

$$\sigma(^{17}\text{F}) = 113.9[1.0^{+0.12}_{-0.05}] \times 10^{-46} \text{ cm}^2, \quad 1\sigma. \tag{35}$$

The maximum neutrino energy is

$$q_\odot = 1.7364 \pm 0.0003 \text{ MeV}, \tag{36}$$

and the average neutrino energy emitted is

$$\langle q_\odot \rangle = 997.7 \text{ keV}. \tag{37}$$

IX. *hep* NEUTRINOS

The calculations for the rare *hep* solar neutrinos are analogous to the calculations for the ^{8}B neutrinos, which are discussed in Sec. VIII A except that the thermal energy shift given in Eq. (19) must be included for the *hep* neutrinos. I find

$$\sigma(hep) = 7.14[1.0^{+0.32}_{-0.16}] \times 10^{-42} \text{ cm}^2, \quad 1\sigma. \tag{38}$$

Only 7% of the best-estimate cross section is from ground-state to ground-state transitions.

The maximum neutrino energy is

$$q_\odot = 18.778 \text{ MeV}, \tag{39}$$

and the average neutrino energy is

$$\langle q_\odot \rangle = 9.628 \text{ MeV}. \tag{40}$$

X. ^{7}Be, *pep*, AND ^{37}Ar ABSORPTION CROSS SECTIONS

In this section, I present the calculated cross sections for the solar neutrino lines from ^{7}Be electron capture and from the *pep* process, electron capture during the *pp* reaction. I also calculate the cross section for absorption of neutrinos from a ^{37}Ar laboratory radioactive source, which emits a neutrino with a similar energy to the dominant neutrino line from ^{7}Be electron capture in the Sun.

A. Neutrino line from ^{7}Be electron capture

The ^{7}Be neutrinos are the second most significant contributor to the calculated event rates in gallium neutrino experiments, according to the predictions [14] of the standard solar model and the standard electroweak theory. The best-estimate cross section, weighted according to the branching ratios indicated in Eq. (21) and Eq. (22), is

$$\sigma(^7\text{Be}) = 71.7[1.0^{+0.07}_{-0.03}] \times 10^{-46} \text{ cm}^2, \quad 1\sigma, \tag{41}$$

which is about 2% smaller than calculated previously [13]. The inclusion of the thermal energy of the interacting electron and ^{7}Be ion [cf. Eqs. (21) and (22)] increases the cross section by only 0.2%. Excited state transitions contribute approximately 6% of the total best-estimate cross section given in Eq. (41).

The uncertainties given in Eq. (41) represent, at the 3σ limit, extreme values. The 3σ lower limit (-9%) was obtained by setting equal to zero all excited state contributions and by decreasing the best-estimate cross section by 3 times the calculated contribution from forbidden corrections. The uncertainties were added in quadratures. The 3σ upper limit ($+21\%$) corresponds to maximizing the BGT value allowed, at 3σ, by the experimental constraint, Eq. (14), on the observed capture rate from chromium neutrinos. This maximization is equivalent to multiplying by seven the (p,n) estimate for the BGT value leading to the 500 keV excited state in ^{71}Ge (see Anselmann *et al.* [3] for a similar argument using the initial results of the GALLEX source experiment). The smaller uncertainty due to forbidden corrections, 2.4% (1σ), was combined quadratically with the excited state uncertainty.

B. Neutrino line from the *pep* electron capture reaction

The flux of *pep* neutrinos is about 400 times less than the flux of *pp* neutrinos [14]. Hence, it is not necessary to know accurately the cross section for *pep* neutrino absorption by ^{71}Ga, which is fortunate since the uncertainties, dominated primarily by the unknown strengths of transitions to excited states, are relatively large.

The best-estimate cross section for the *pep* reaction is

$$\sigma(pep) = 204[1.0^{+0.17}_{-0.07}] \times 10^{-46} \text{ cm}^2, \quad 1\sigma, \tag{42}$$

which is about 5% smaller than calculated previously [13]. Much of this change is due to uncertainty in where to locate the (p,n) transition strength that was found experimentally [23,26] to be somewhere between 1.0 MeV and 1.50 MeV

excitation energy in ^{71}Ge. In my earlier calculations [13,14], I assumed that this transition strength was centered on the 1.095 MeV excited state in ^{71}Ge. For the calculations in this paper, I have assumed that strength is located at about 1.25 MeV, at the midpoint of the experimentally allowed region and close to the exited state at 1.30 MeV excitation energy in ^{71}Ge. Moving the presumed location of this transition strength from an assumed excitation energy of 1.25 MeV to an excitation energy of 1.10 MeV increases the calculated cross section by 3.8%.

About 18% of the best-estimate cross section arises from excited state transitions.

The 3σ lower limit is determined by setting equal to zero the cross sections for all excited state transitions and by multiplying by 3 the change in the cross section that results from ignoring all forbidden corrections. The 3σ upper limit was determined by (1) allowing the maximum contribution from the first two excited states of ^{71}Ge that is consistent with the constraint [see Eq. (14)] from the ^{71}Cr experiment, (2) locating at 1.10 MeV (the lowest possible energy) the excitation strength to ^{71}Ge excited states observed to be between 1.0 MeV and 1.50 MeV excitation energy, and (3) doubling the BGT value determined from the (p,n) reactions for the other relevant excited states. The different contributions to the uncertainty embodied in the 3σ upper limit were added quadratically.

The amount of thermal energy that the combining electron and two protons contribute, on the average, to the pep neutrino energy has not been calculated accurately. Fortunately, this is unimportant for our purposes. The neutrino end point energy neglecting thermal energies is known precisely and is 1.442 232 MeV, when account is taken of the extra 13.6 eV binding energy that is included in the tabulations of the neutral atoms masses. If we augment this nuclear mass difference by the same amount of thermal energy, 5 keV, as for the pp reaction, which is a plausible approximation, we obtain

$$q_{\odot} \approx 1.445 \ \ \text{MeV} \ . \tag{43}$$

The best-estimate cross section given in Eq. (42) was calculated using the approximate neutrino energy given in Eq. (43). The calculated cross section is decreased by only 0.6%, of negligible importance for solar neutrino experiments, if the entire estimated 5 keV thermal energy is dropped.

C. Neutrino line from ^{37}Ar electron capture in the laboratory

Haxton [44] has suggested using a laboratory radioactive source of ^{37}Ar to test the efficiency of radiochemical solar neutrino detectors. The neutrino energy of the ^{37}Ar K-shell decay is 0.811 MeV; the L-shell energy is 0.813 MeV. Thus neutrinos from ^{37}Ar decay in the laboratory have energies within several percent of the energy [863 keV; see Eq. (21)] of the dominant ^{7}Be line. As Haxton has emphasized, an experiment carried out with an intense ^{37}Ar source would therefore provide a valuable additional test of the overall efficiency of gallium detectors in observing the important ^{7}Be neutrinos.

The calculation of the absorption cross section for ^{37}Ar neutrinos is very similar to the calculation of the absorption cross section for ^{7}Be neutrinos described in Sec. X A. I find

$$\sigma(^{37}\text{Ar}) = 70.0[1.0^{+0.07}_{-0.03}] \times 10^{-46} \ \text{cm}^2, \ \ 1\sigma, \tag{44}$$

which agrees well with the previously published value of 72×10^{-46} cm^2 [14]. The calculated total cross sections for ^{37}Ar and ^{7}Be neutrinos differ by only 2.4% [cf. Eq. (41) and Eq. (44)]. As stressed by Haxton, if one varies the assumed energy of the dominant excited state transition, the ^{37}Ar neutrino absorption cross section tracks the cross section for ^{7}Be neutrinos remarkably well. Considering three extreme cases, i.e., no excited state transitions, the maximum allowed strength for the transition to the 175 keV excited state, and the maximum allowed strength to the 500 keV excited state, the total spread in the ratio of the ^{7}Be to the ^{37}Ar neutrino absorption cross sections is only 0.6%.

The contributions of the two energetically—allowed transitions to excited states of ^{71}Ge (see Fig. 1) are proportional to the BGT values for those excited state transitions. Thus one can write

$$\sigma(^{37}\text{Ar}) = \left[66.2 + 46.0\frac{\text{BGT}(175 \text{ keV})}{\text{BGT}_{\text{g.s.}}} \right.$$
$$\left. + 17.4\frac{\text{BGT}(500 \text{ keV})}{\text{BGT}_{\text{g.s.}}} \right] \times 10^{-46} \ \text{cm}^{-2} \ . \tag{45}$$

The best-estimate cross section given in Eq. (44) was obtained by using in Eq. (45) the BGT values indicated by (p,n) reactions (see Sec. II and Table I). Excited state transitions contribute 5% of the best-estimate cross section for ^{37}Ar neutrinos, very similar to the 6% contributed by excited states to the best-estimate ^{7}Be neutrino absorption cross section. The uncertainties in the calculated cross section that are shown in Eq. (44) were calculated in the same way as for the ^{7}Be line (see Sec. X A).

XI. ABSORPTION CROSS SECTIONS AT SPECIFIC ENERGIES

Neutrino absorption cross sections at specific energies are required in order to calculate the capture rates predicted by different scenarios with new physics (e.g., neutrino oscillations with a variety of mixing parameters) in which the energy spectrum of solar neutrinos is changed from the standard neutrino energy spectrum. In this section, I provide the required cross sections as a function of energy and, for the first time, also present the uncertainties in the cross sections as a function of energy.

Table II gives the best-estimate neutrino cross sections at a set of strategically chosen energies. The cross sections were evaluated according to the precepts described in the previous sections. Using a cubic spline fit [45] to the cross sections as a function of energy that are given in Table II, I have verified that the numbers given in the table are sufficient to reproduce to an accuracy of 1% or better the best-estimate cross sections calculated in the previous sections for the standard neutrino energy spectra.

The uncertainties in the neutrino cross sections depend upon neutrino energy since the number of accessible excited states increases with energy and the forbidden corrections

TABLE II. Best-estimate absorption cross sections for specific energies. The energies q are expressed in MeV and the cross sections σ, in units of 10^{-46} cm^2.

q	σ	q	σ	q	σ
0.240	1.310×10^1	1.500	2.243×10^2	10.000	5.710×10^4
0.250	1.357×10^1	1.600	2.553×10^2	10.500	6.705×10^4
0.275	1.499×10^1	1.700	2.886×10^2	11.000	7.781×10^4
0.300	1.662×10^1	1.750	3.061×10^2	11.500	8.937×10^4
0.325	1.836×10^1	2.000	3.972×10^2	12.000	1.017×10^5
0.350	2.018×10^1	2.500	6.493×10^2	12.500	1.148×10^5
0.375	2.208×10^1	3.000	9.905×10^2	13.000	1.287×10^5
0.400	2.406×10^1	3.500	1.464×10^3	13.500	1.432×10^5
0.425	2.648×10^1	4.000	2.129×10^3	14.000	1.585×10^5
0.450	2.862×10^1	4.500	3.074×10^3	14.500	1.745×10^5
0.500	3.314×10^1	5.000	4.380×10^3	15.000	1.912×10^5
0.600	4.300×10^1	5.500	6.133×10^3	15.500	2.085×10^5
0.700	5.397×10^1	6.000	8.434×10^3	16.000	2.264×10^4
0.800	6.848×10^1	6.500	1.144×10^4	18.000	3.040×10^5
0.900	8.276×10^1	7.000	1.530×10^4	20.000	3.899×10^5
1.000	9.830×10^1	7.500	2.009×10^4	22.500	5.064×10^5
1.100	1.226×10^2	8.000	2.576×10^4	25.000	6.296×10^5
1.200	1.440×10^2	8.500	3.230×10^4	30.000	8.789×10^5
1.300	1.672×10^2	9.000	3.968×10^4		
1.400	1.921×10^2	9.500	4.797×10^4		

TABLE III. The 3σ lower-limit cross sections. The energies q are expressed in MeV and the cross sections σ in units of 10^{-46} cm^2.

q	σ	q	σ	q	σ
0.240	1.224×10^1	1.500	1.882×10^2	10.000	3.040×10^4
0.250	1.268×10^1	1.600	2.122×10^2	10.500	3.541×10^4
0.275	1.400×10^1	1.700	2.378×10^2	11.000	4.082×10^4
0.300	1.551×10^1	1.750	2.511×10^2	11.500	4.657×10^4
0.325	1.714×10^1	2.000	3.162×10^2	12.000	5.264×10^4
0.350	1.884×10^1	2.500	4.971×10^2	12.500	5.902×10^4
0.375	2.060×10^1	3.000	7.318×10^2	13.000	6.568×10^4
0.400	2.244×10^1	3.500	1.041×10^3	13.500	7.260×10^4
0.425	2.465×10^1	4.000	1.456×10^3	14.000	7.973×10^4
0.450	2.664×10^1	4.500	2.017×10^3	14.500	8.706×10^4
0.500	3.083×10^1	5.000	2.766×10^3	15.000	9.455×10^4
0.600	3.996×10^1	5.500	3.744×10^3	15.500	1.022×10^5
0.700	5.011×10^1	6.000	5.001×10^3	16.000	1.098×10^5
0.800	6.245×10^1	6.500	6.615×10^3	18.000	1.406×10^5
0.900	7.505×10^1	7.000	8.658×10^3	20.000	1.689×10^5
1.000	8.868×10^1	7.500	1.117×10^4	22.500	1.955×10^5
1.100	1.076×10^2	8.000	1.412×10^4	25.000	2.056×10^5
1.200	1.251×10^2	8.500	1.752×10^4	30.000	1.484×10^5
1.300	1.439×10^2	9.000	2.136×10^4		
1.400	1.640×10^2	9.500	2.566×10^4		

also increase with energy. The energy dependence of the cross section uncertainties has not, so far as I know, been taken into account in the previously published comparisons of the calculated and observed rates in neutrino experiments. In order to provide the data with which to include the energy-dependent cross section uncertainties in future analyses, I have combined quadratically the uncertainties from different sources, as indicated in the discussion in the previous sections, and have calculated 3σ upper and lower limit cross sections at the same energies at which cross sections are listed in Table II.

The 3σ limit cross sections are given in Table III and Table IV. I have also verified that a cubic spline fit to the cross sections given in these tables may be used to evaluate the cross section uncertainties in the rates predicted by physics scenarios with nonstandard neutrino energy spectra. (Figure 4, below, shows the calculated cross sections and the estimated 3σ uncertainties as a function of neutrino energy. For energies above 25 MeV, the uncertainties become so large as to make the calculated cross sections not very useful.)

XII. PREDICTED SOLAR NEUTRINO EVENT RATES

The event rates measured by the GALLEX [1] and SAGE [2] solar neutrino experiments are significantly less than the standard solar model predictions if nothing happens to the neutrinos after they are produced in the center of the Sun. How can we assess the significance of this deficit?

Over the years, I have given a formal quantitative measure of the reliability of the theoretical predictions by determining errors in the calculations based upon the recognized uncertainties in the input data. This work has been published

largely in the Reviews of Modern Physics and the investigations prior to 1989 are summarized in Neutrino Astrophysics [14] (for recent improvements see [41] and [42]).

In this section, I provide two different ways of assessing the robustness of the theoretical predictions. In Sec. XII A, I review all of the published standard solar model calculations since 1963 in which my colleagues and I have been involved. The variation over time of the standard model neutrino fluxes provides an intuitive feeling for the reliability of the theoretical calculations. In Sec. XII B, I present the results of a series of new solar model calculations in which different nuclear reaction rates are set equal to zero in order to minimize artificially the calculated total event rate for gallium neutrino experiments. These solar model *gedanken* experiments provide a different indication of how difficult it is to lower significantly the predicted solar model event rates.

A. Standard solar model predictions

Figure 3 shows the event rates computed for all the neutrino fluxes predicted by the then best standard solar models which I and my collaborators have published since the first such model appeared in 1963 [46]. To isolate the effects of solar models, the rates shown in Fig. 3 were computed in all cases with the absorption cross sections determined in the present paper for standard solar neutrino energy spectra. The uncertainties indicated in Fig. 3 are the 1σ errors due just to the cross section uncertainties estimated in the present paper. I have assumed that the uncertainties from different excited state transitions add linearly and coherently; i.e., the cross sections for the individual neutrino sources are simultaneously increased (or decreased) to their maximum (minimum) allowed values.

TABLE IV. The 3σ maximum cross sections. The energies q are expressed in MeV and the cross sections σ in units of 10^{-46} cm^2.

q	σ	q	σ	q	σ
0.240	1.395×10^1	1.500	3.311×10^2	10.000	1.123×10^5
0.250	1.446×10^1	1.600	3.829×10^2	10.500	1.321×10^5
0.275	1.598×10^1	1.700	4.390×10^2	11.000	1.536×10^5
0.300	1.772×10^1	1.750	4.685×10^2	11.500	1.766×10^5
0.325	1.958×10^1	2.000	6.336×10^2	12.000	2.013×10^5
0.350	2.153×10^1	2.500	1.073×10^3	12.500	2.275×10^5
0.375	2.357×10^1	3.000	1.688×10^3	13.000	2.552×10^5
0.400	2.567×10^1	3.500	2.559×10^3	13.500	2.845×10^5
0.425	3.101×10^1	4.000	3.808×10^3	14.000	3.152×10^5
0.450	3.362×10^1	4.500	5.609×10^3	14.500	3.474×10^5
0.500	3.921×10^1	5.000	8.127×10^3	15.000	3.811×10^5
0.600	5.154×10^1	5.500	1.153×10^4	15.500	4.161×10^5
0.700	6.534×10^1	6.000	1.603×10^4	16.000	4.526×10^5
0.800	8.261×10^1	6.500	2.194×10^4	18.000	6.117×10^5
0.900	1.031×10^2	7.000	2.954×10^4	20.000	7.910×10^5
1.000	1.258×10^2	7.500	3.900×10^4	22.500	1.041×10^6
1.100	1.658×10^2	8.000	5.022×10^4	25.000	1.317×10^6
1.200	1.996×10^2	8.500	6.316×10^4	30.000	1.930×10^6
1.300	2.366×10^2	9.000	7.779×10^4		
1.400	2.768×10^2	9.500	9.422×10^4		

The predicted neutrino fluxes have been remarkably constant in time over the last three decades. Prior to this time, in the first several years of solar neutrino studies that are represented by the earliest points in Fig. 3, the cross sections for the low energy nuclear physics reactions were not well known and the reaction rates calculated with the then-current nuclear cross sections led to large values for the higher-energy, more easily detectable neutrinos. In 1964, when the chlorine solar neutrino experiment was proposed [47,48], the rate of the ^{3}He-^{3}He reaction was estimated [49,50] to be 5 times slower than the current best estimate and the uncertainty in the low-energy cross section was estimated [50] to be "as much as a factor of 5 or 10." Since the ^{3}He-^{3}He reaction competes with the ^{3}He-^{4}He reaction—which leads to high-energy neutrinos—the calculated fluxes for the higher energy neutrinos were overestimated in the earliest days of solar neutrino research. The most significant uncertainties, in the rates of the ^{3}He-^{3}He, the ^{3}He-^{4}He, and the ^{7}Be-p reactions, were much reduced after just a few years of intensive experimental research in the middle and late 1960s [51].

The event rates for gallium appear even more robust when account is taken of the fact that prior to 1992 the standard solar models did not include the effects of diffusion. Using cross sections calculated in this paper and neutrino fluxes predicted by the 1995 Bahcall-Pinsonneault [42] standard model (which includes helium and heavy element diffusion and the 1995 best estimates for the nuclear reaction rates), as well as recent improvements in radiative opacity and equation of state [52], the calculated event rate is

standard solar model capture rate with diffusion
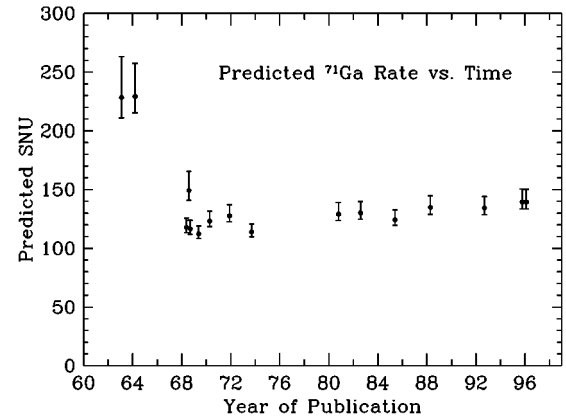
$$= 135 \quad \text{SNU}, \tag{46}$$

FIG. 3. Predicted solar neutrino gallium event rate versus year of publication. The figure shows the event rates for all of the standard solar model calculations that my colleagues and I have published [41,42,46,52,56]. The cross sections from the present paper have been used in all cases to convert the calculated neutrino fluxes to predicted capture rates. The estimated 1σ uncertainties reflect in all cases just the uncertainties in the cross sections that are evaluated in the present paper. For the 35 years over which we have been calculating standard solar model neutrino fluxes, the historically lowest value (fluxes published in 1969) corresponds to 109.5 SNU. This lowest-ever value is 5.6σ greater than the combined GALLEX and SAGE experimental result. If the points prior to 1992 are increased by 11 SNU to correct for diffusion (this was not done in the figure), then all of the standard model theoretical capture rates since 1968 through 1997 lie in the range 120 SNU to 141 SNU, i.e., (131 ± 11) SNU.
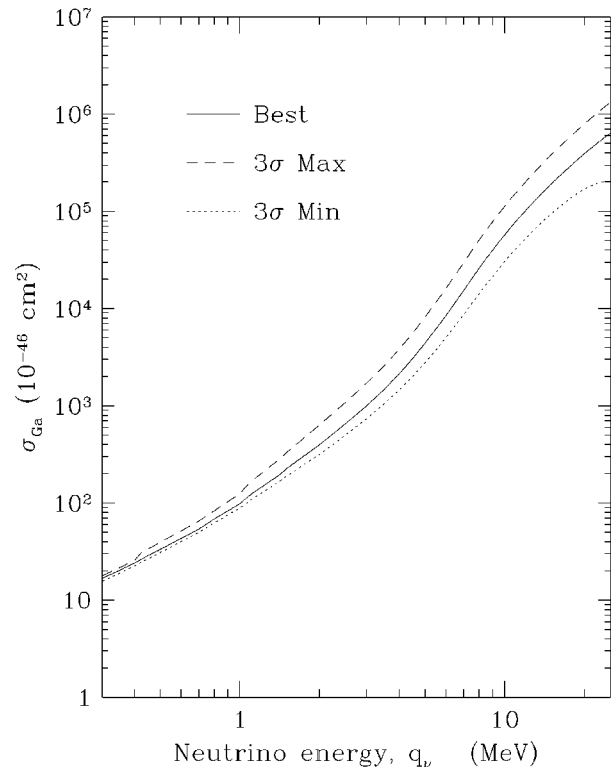

FIG. 4. Absorption cross sections for gallium as a function of energy. The figure displays the best-estimate cross sections as well as the $\pm3\sigma$ cross sections. Numerical values are given in Table II, Table III, and Table IV.

1 SNU less than calculated with the previously used cross sections [42]. Omitting diffusion, but otherwise using all the same code and data to construct a standard solar model [42], the calculated rate with the gallium cross sections given in this paper is

standard solar model capture rate without diffusion

$$= 124 \text{ SNU}. \tag{47}$$

Comparing the results given in Eq. (46) and Eq. (47), we see that the effect of including diffusion is to increase by about 11 SNU the standard solar model prediction for the gallium solar neutrino event rate.

Helioseismological measurements show that element diffusion is occurring in the Sun, confirming theoretical expectations. The present-day surface abundance of helium calculated from solar models is in excellent agreement with the helioseismologically determined value only if diffusion is included [42]; the comparison of the computed and observed depth of the convective zone also requires that diffusion be included in the solar models [41,42]. More recently, it has been shown [52] that the sound velocities of the Sun determined by helioseismological measurements from $0.05 R_{\odot}$ to $0.95 R_{\odot}$ agree to within 0.1% rms with the sound velocities calculated from a standard solar model provided that diffusion is included in the model calculations. The mean-squared discrepancy for a model without diffusion is 22 times larger than for the standard model with diffusion, indicating that models without diffusion are inconsistent with helioseismological measurements [52].

If the values prior to 1992 in Fig. 3 are increased by 11 SNU to correct for the omission of diffusion, then the corrected values since 1968 through 1997 all lie in the range 120 SNU to 141 SNU, i.e.,

total historical range corrected for diffusion

$$= 120 \text{ SNU} - 141 \text{ SNU}, \quad 1968 - 1997. \tag{48}$$

The observed event rate in the GALLEX detector is [1]

$$\text{GALLEX observation} = 70 \pm 8 \text{ SNU}, \tag{49}$$

and the rate observed by the SAGE detector is [2]

$$\text{SAGE observation} = 72 \pm 13 \text{ SNU}. \tag{50}$$

The weighted average observed rate is 70.5 ± 7 SNU.

The difference between the predicted rate, Eq. (46), and the observed rates, Eq. (49) and Eq. (50), is the essence of the contemporary gallium solar neutrino problem. Moreover, the GALLEX observation is, by itself, more than 5σ below all the standard solar model results shown in Fig. 3 since 1968, if the values prior to 1992 are corrected for the effects of diffusion.

B. Models with selected nuclear reaction rates set equal to zero

The neutrino absorption cross sections are a monotonically increasing function of energy (cf. Table II). Therefore, the minimum conceivable event rate is achieved if one artificially sets equal to zero the nuclear reactions that produce

TABLE V. The minimum solar neutrino rates if selected nuclear reactions are set equal to zero. The 1σ uncertainty in the chlorine rate is about ± 0.01 SNU in all three cases.

Reactions set equal to zero		Ga rate (SNU)	Cl rate (SNU)
$^3\text{He}(\alpha, \gamma)^7\text{Be}$		$88.1^{+3.2}_{-2.4}$	0.7
$^3\text{He}(\alpha, \gamma)^7\text{Be}$,	$^{12}\text{C}(p, \gamma)^{13}\text{N}$	$79.7^{+2.4}_{-2.0}$	0.3
$^3\text{He}(\alpha, \gamma)^7\text{Be}$,	all CNO reactions	$79.5^{+2.3}_{-2.0}$	0.3

higher-energy neutrinos, like the ^7Be, ^8B, and CNO neutrinos. The first such calculation was performed by Bahcall, Cleveland, and Davis [53], who minimized the rate subject only to the condition that the nuclear energy released by fusion in the solar interior equal the present-day solar luminosity. Allowing only pp and pep neutrinos and using the previous best estimates for gallium neutrino absorption cross sections, these authors obtained a minimum allowed rate— for standard neutrino physics—of 80 SNU.

In Table V, I summarize the results of a series of solar model calculations that were made by setting equal to zero selected nuclear reactions. The models were constructed in the same way as the best Bahcall-Pinsonneault solar models [42], except that specific nuclear reactions were artificially set equal to zero in the nuclear energy generation subroutine.

The most dramatic decrease in the predicted gallium event rate is achieved by setting to zero the rate of the well-known $^3\text{He}(^4\text{He}, \gamma)^7\text{Be}$ reaction, which leads in the standard solar model to the neutrinos from ^7Be electron and proton capture, the so-called ^8B and ^7Be neutrinos. With this reaction equal to zero, the only way in the pp chain of completing the fusion of protons into alpha particles is by the low-energy pp reaction, with an occasional ($\sim 0.2\%$ by neutrino flux) pep reaction.

The calculated event rate is

$$\text{no } ^3\text{He}(^4\text{He}, \gamma)^7\text{Be reactions} = 88.1^{+3.2}_{-2.4} \text{ SNU}, \tag{51}$$

with 1σ errors on the neutrino absorption cross sections. The corresponding rate in the chlorine solar neutrino experiment is 0.73 ± 0.01 SNU, which is more than 10σ less than the observed rate [54] of 2.54 ± 0.20 SNU. The rate, 0.0 SNU, predicted for the Kamiokande solar neutrino experiment is 8σ less than the observed rate in the Kamiokande experiment [55]. Nevertheless, the gallium event rate of 88 SNU calculated in this concocted (clearly incorrect) model is about 2.5 standard deviations larger than the combined observed rate of 70.5 SNU in the GALLEX and SAGE experiments.

The primary reason that the rate given here is larger than the value calculated by Bahcall, Cleveland, and Davis [53] is that some of the solar luminosity and neutrinos are coming from the CNO fusion reactions. The calculated event rate in the gallium experiments can be reduced somewhat further if one sets equal to zero simultaneously the rates of both the $^3\text{He}(^4\text{He}, \gamma)^7\text{Be}$ reaction and the $^{12}\text{C}(p, \gamma)^{13}\text{N}$ reactions. In this case, the CNO neutrinos (from ^{13}N, ^{15}O, and ^{17}F decays) are all greatly reduced in flux and the ^7Be and ^8B neutrinos are completely absent. Table V shows the the calculated rate for this case is $79.7^{+2.4}_{-2.0}$ SNU.

TABLE VI. Neutrino absorption cross sections for standard energy spectra. All cross sections are given in units of 10^{-46} cm^2 except for ^{8}B and hep neutrinos, for which the unit is 10^{-42} cm^2. The uncertainties indicated are effective 1σ uncertainties.

Source	pp	pep	hep	^{7}Be	^{8}B	^{13}N	^{15}O	^{17}F	^{37}Ar	^{51}Cr
Best	11.72	204	7.14	71.7	2.40	60.4	113.7	113.9	70.0	58.1
$1\sigma_+(\%)$	2.3	17	32	7	32	6	12	12	0.07	0.04
$1\sigma_-(\%)$	2.3	7	16	3	15	3	6	6	0.03	0.03

The minimum rate is achieved by simultaneous setting equal to zero the reaction rates for the ^{3}He(^{4}He, γ)^{7}Be reaction and *all* the CNO reactions.[2] In this case, I find

$$\text{minimum rate} = 79.5^{+2.3}_{-2.0} \text{ SNU}, \qquad (52)$$

where the uncertainties are again 1σ errors. This extreme hypothesis also predicts 0.0 SNU for the Kamiokande experiment and 0.3 SNU for the ^{37}Cl experiment; the latter value is 11 standard deviations less than the observed capture rate in the chlorine detector [54].

The solar neutrino fluxes that produce the minimum neutrino capture rate in gallium detectors are $\phi(pp) = 6.50 \times 10^{10}$ cm^{-2} s^{-1}, $\phi(pep) = 1.61 \times 10^8$ cm^{-2} s^{-1}, and $\phi(hep) = 1.4 \times 10^3$ cm^{-2} s^{-1}.

XIII. SUMMARY AND DISCUSSION

I first summarize the calculations of neutrino absorption cross sections and then discuss the event rates predicted by standard solar models and by extremely nonstandard solar models. In the last subsection, I suggest an answer to the question, what will GNO show?

I present in Appendix A the standard pp neutrino energy spectrum that was calculated with the inclusion of the thermal energy of fusing ions and also present in Appendix B the standard CNO neutrino energy spectra.

A. Cross sections

1. Best estimates

Table VI summarizes the best estimates and the 1σ uncertainties of the neutrino absorption cross sections that were calculated in the preceding sections for ^{71}Ga targets. All of the cross sections given in Table VI were evaluated assuming standard ν_e energy spectra and the input data for the ^{71}Ga-^{71}Ge system that are summarized in Sec. II. The f value for ^{71}Ge electron capture used here makes use of new Dirac-Fock self-consistent-field calculations of the electron wave functions that include finite nuclear size, the Breit interaction, and the most important QED corrections [20–22]. In addition, I have taken account of atomic overlap and exchange effects (see Sec. III), effects for which I have previously only estimated upper limits.

I have also included here for the first time the thermal energy contribution of the fusing particles to the neutrino absorption cross sections. Section VI presents the results of

calculations of the thermal energy from neutrino-producing reactions that occur in the solar interior. This thermal energy increases by 1.6% the calculated absorption cross section for pp neutrinos, but is unimportant for all other cases considered in this paper.

The cross section for ν_e absorption by ^{51}Cr calculated here agrees to better than 1σ with the independent measurements by the GALLEX [3,4] and SAGE [6] experiments. However, the measured rates in the GALLEX and SAGE solar neutrino experiments differ by more than 5σ from all the standard solar model predictions of my colleagues and myself since 1968 provided the values published prior to 1992 are corrected, as required by helioseismology, for the effects of diffusion (see Sec. XII A).

2. Particle physics applications

Many particle physics explanations of the observed solar neutrino event rates imply that the energy spectrum of ν_e solar neutrinos is altered by new physics. In order to calculate the rates expected from the variety of proposed nonstandard neutrino energy spectra, one must have available neutrino cross sections, and their uncertainties, as a function of neutrino energy. I have not previously published uncertainties in the cross sections calculations as a function of energy. Therefore, in the many papers in which empirical analyses of solar neutrinos were made using nonstandard neutrino energy spectra, the theoretical errors in the cross section calculations were, of necessity, either ignored or (incorrectly) set equal to the published uncertainties for cross sections with standard ν_e energy spectra.

Table II presents the required neutrino cross sections at a set of neutrino energies that were chosen to permit, with the aid of a cubic spline fit, accurate calculations for any specified neutrino energy spectrum. I have also calculated 3σ different minimum and maximum absorption cross sections, which are presented in Table III and Table IV.

Figure 4 displays the cross sections and their uncertainties as a function of neutrino energy. Using the best estimates and 3σ different cross sections given in the tables, one can calculate the uncertainties in predicted neutrino event rates for an arbitrarily changed solar neutrino energy spectrum.

3. Uncertainties

Since gallium solar neutrino experiments test fundamental aspects of physics and astrophysics, I have adopted extremely conservative criteria for the estimated uncertainties. In most cases, the largest uncertainties arise from the poorly known strengths of transitions to excited states in ^{71}Ge.

For low- and moderate-energy neutrino sources, the pp, pep, ^{7}Be, ^{13}N, ^{15}O, and ^{17}F neutrinos, I have set equal to

---

[2]In this case, one requires zero cross sections for ^{3}He(^{4}He, γ)^{7}Be, ^{12}C(p, γ)^{13}N, ^{13}C(p, γ)^{14}N, ^{14}N(p, γ)^{15}O, and ^{15}N(p, γ)^{16}O.

TABLE VII. The pp neutrino spectrum. The normalized pp neutrino energy spectrum $P(q)$ is given in intervals of 5.0406 keV. The neutrino energy, q, is expressed in MeV and $P(q)$ is normalized per MeV.

q	$P(q)$	q	$P(q)$	q	$P(q)$	q	$P(q)$
0.00504	0.0035	0.11089	1.2477	0.21675	3.2300	0.32260	4.0356
0.01008	0.0138	0.11593	1.3417	0.22179	3.3094	0.32764	4.0114
0.01512	0.0307	0.12097	1.4370	0.22683	3.3859	0.33268	3.9794
0.02016	0.0538	0.12601	1.5335	0.23187	3.4594	0.33772	3.9391
0.02520	0.0830	0.13106	1.6310	0.23691	3.5298	0.34276	3.8900
0.03024	0.1179	0.13610	1.7291	0.24195	3.5966	0.34780	3.8316
0.03528	0.1582	0.14114	1.8278	0.24699	3.6599	0.35284	3.7632
0.04032	0.2038	0.14618	1.9267	0.25203	3.7194	0.35788	3.6842
0.04537	0.2543	0.15122	2.0258	0.25707	3.7749	0.36292	3.5937
0.05041	0.3094	0.15626	2.1247	0.26211	3.8262	0.36796	3.4907
0.05545	0.3691	0.16130	2.2233	0.26715	3.8731	0.37300	3.3740
0.06049	0.4329	0.16634	2.3214	0.27219	3.9154	0.37804	3.2422
0.06553	0.5006	0.17138	2.4187	0.27723	3.9529	0.38309	3.0932
0.07057	0.5721	0.17642	2.5151	0.28227	3.9854	0.38813	2.9246
0.07561	0.6469	0.18146	2.6105	0.28731	4.0127	0.39317	2.7330
0.08065	0.7250	0.18650	2.7044	0.29235	4.0344	0.39821	2.5136
0.08569	0.8061	0.19154	2.7969	0.29740	4.0505	0.40325	2.2589
0.09073	0.8899	0.19658	2.8877	0.30244	4.0605	0.40829	1.9567
0.09577	0.9761	0.20162	2.9766	0.30748	4.0644	0.41333	1.5832
0.10081	1.0647	0.20666	3.0634	0.31252	4.0617	0.41837	1.0783
0.10585	1.1553	0.21171	3.1479	0.31756	4.0522	0.42341	0.0000

zero the matrix elements for all excited state transitions in order to determine the 3σ minimum cross sections. I have calculated the 3σ upper limit for the important transitions to the 175 keV and the 500 keV states in ^{71}Ge (see Fig. 2), by using the constraint from the GALLEX [3–5] and SAGE [6] measurements of the ^{51}Cr absorption rate [see Eq. (14)]. This prescription results in 3σ upper limit cross sections that are, respectively, 7 and 12 times the values inferred using the measured (p,n) cross sections (see discussion in Sec. IV E), which are probably unrealistically large uncertainties since the BGT values inferred from (p,n) measurements have never been observed to exceed by large factors the true BGT values determined by beta-decay experiments.

I have also taken a skeptical attitude toward the calculated values of the forbidden corrections, and have adopted 1σ uncertainties from forbidden effects equal to the best-estimate values for the forbidden corrections. For the low- and moderate-energy neutrino sources, the forbidden corrections are always between 2% and 2.5%. The 1σ uncertainties estimated in this way are significant for the pp, ^{7}Be, ^{13}N, ^{37}Ar, and ^{51}Cr neutrino cross sections (cf. Table VI) but, with the exception of the pp cross section, only for the lower limit value.

The largest uncertainties in the ^{51}Cr calculation are from excited state transitions ($+2.8\%$ and -1.6%, 1σ) and forbidden corrections ($\pm 2.3\%$, 1σ). I have also calculated the cross section for absorption of ^{37}Ar neutrinos, since, as Haxton [44] has discussed, the close similarity between the ^{37}Ar and ^{7}Be neutrino energies makes argon a theoretically attractive possible calibrator for the detection efficiency for ^{7}Be neutrinos.

4. Correlations among the uncertainties

How are the uncertainties correlated between cross sections calculated for different energies? Some of the sources of uncertainties are fully correlated; e.g., the characteristic σ_0 defined by Eq. (3) and Eq. (4) is a common scale factor for all the cross sections. On the other hand, some sources of uncertainties are uncorrelated; uncertainties in matrix elements to highly excited states in ^{71}Ge affect the cross sections for higher-energy neutrinos but do not influence the cross sections for lower-energy neutrinos.

I recommend the most conservative procedure: Assume all errors are fully correlated and add the uncertainties linearly not quadratically. This is the procedure that I have followed in calculating Table III and Table IV. For standard model predictions, i.e., standard solar models and nonoscillating neutrinos, adding the uncertainties linearly and quadratically will give approximately the same answer because the uncertainties are dominated by the higher-energy neutrinos from ^{8}B. However, for nonstandard neutrino scenarios, such as the MSW effect or vacuum neutrino oscillations, the two procedures may give significantly different results. To test for the sensitivity of the error estimate to the prescription adopted, one can combine the errors quadratically and also linearly and compare the difference error estimates. In certain cases, it may be reasonable to break up the calculations into different energy groups, e.g., below or above 2 MeV, and assume that the uncertainties are correlated within each group but not between groups.

B. Predicted event rates

Figure 3 shows the event rates calculated using all of the standard solar model neutrino fluxes that my colleagues and

TABLE VIII. The ^{13}N neutrino spectrum. The normalized ^{13}N neutrino energy spectrum $P(q)$ is given in intervals of 14.264 keV. The neutrino energy q is expressed in MeV and $P(q)$ is normalized per MeV.

q	$P(q)$	q	$P(q)$	q	$P(q)$	q	$P(q)$
0.01426	0.0018	0.31381	0.5787	0.61336	1.2865	0.91291	1.2732
0.02853	0.0071	0.32808	0.6185	0.62763	1.3066	0.92718	1.2472
0.04279	0.0157	0.34234	0.6583	0.64189	1.3248	0.94144	1.2186
0.05706	0.0275	0.35661	0.6981	0.65616	1.3413	0.95571	1.1875
0.07132	0.0422	0.37087	0.7378	0.67042	1.3558	0.96997	1.1538
0.08559	0.0596	0.38514	0.7771	0.68469	1.3684	0.98424	1.1175
0.09985	0.0796	0.39940	0.8160	0.69895	1.3790	0.99850	1.0784
0.11411	0.1020	0.41366	0.8544	0.71321	1.3876	1.01276	1.0366
0.12838	0.1267	0.42793	0.8922	0.72748	1.3940	1.02703	0.9918
0.14264	0.1534	0.44219	0.9293	0.74174	1.3983	1.04129	0.9440
0.15691	0.1820	0.45646	0.9656	0.75601	1.4005	1.05556	0.8931
0.17117	0.2124	0.47072	1.0010	0.77027	1.4005	1.06982	0.8387
0.18544	0.2444	0.48499	1.0353	0.78454	1.3983	1.08409	0.7805
0.19970	0.2777	0.49925	1.0686	0.79880	1.3937	1.09835	0.7183
0.21396	0.3124	0.51351	1.1008	0.81306	1.3870	1.11261	0.6512
0.22823	0.3482	0.52778	1.1316	0.82733	1.3778	1.12688	0.5785
0.24249	0.3849	0.54204	1.1612	0.84159	1.3664	1.14114	0.4987
0.25676	0.4226	0.55631	1.1893	0.85586	1.3526	1.15541	0.4094
0.27102	0.4609	0.57057	1.2160	0.87012	1.3364	1.16967	0.3057
0.28529	0.4997	0.58484	1.2411	0.88439	1.3178	1.18394	0.1766
0.29955	0.5391	0.59910	1.2646	0.89865	1.2967	1.19820	0.0000

I have published since the first solar model calculation of neutrino fluxes in 1963. In order to isolate the effect of the solar model predictions, I have used the absorption cross sections derived in this paper for all the points plotted. The event rates have been remarkably constant, especially since 1968, by which time the largest initial uncertainties in determining the nuclear fusion cross sections were greatly reduced [51].

In the 35 years that we have been calculating neutrino fluxes from standard solar models, many improvements have

TABLE IX. The ^{15}O neutrino spectrum. The normalized ^{15}O neutrino energy spectrum $P(q)$ is given in intervals of 20.615 keV. The neutrino energy q is expressed in MeV and $P(q)$ is normalized per MeV.

q	$P(q)$	q	$P(q)$	q	$P(q)$	q	$P(q)$
0.02062	0.0014	0.45354	0.4372	0.88647	0.9227	1.31939	0.8354
0.04123	0.0056	0.47416	0.4663	0.90708	0.9341	1.34001	0.8136
0.06185	0.0123	0.49477	0.4954	0.92770	0.9441	1.36062	0.7902
0.08246	0.0214	0.51539	0.5242	0.94831	0.9527	1.38124	0.7652
0.10308	0.0328	0.53600	0.5528	0.96893	0.9597	1.40185	0.7386
0.12369	0.0463	0.55662	0.5810	0.98954	0.9652	1.42247	0.7106
0.14431	0.0617	0.57723	0.6088	1.01016	0.9692	1.44308	0.6809
0.16492	0.0790	0.59785	0.6360	1.03077	0.9716	1.46370	0.6497
0.18554	0.0979	0.61846	0.6626	1.05139	0.9725	1.48431	0.6170
0.20615	0.1184	0.63908	0.6886	1.07200	0.9717	1.50493	0.5827
0.22677	0.1402	0.65970	0.7138	1.09262	0.9693	1.52555	0.5467
0.24739	0.1634	0.68031	0.7381	1.11324	0.9653	1.54616	0.5091
0.26800	0.1876	0.70093	0.7616	1.13385	0.9596	1.56678	0.4697
0.28862	0.2129	0.72154	0.7840	1.15447	0.9523	1.58739	0.4283
0.30923	0.2391	0.74216	0.8055	1.17508	0.9434	1.60801	0.3846
0.32985	0.2660	0.76277	0.8259	1.19570	0.9329	1.62862	0.3384
0.35046	0.2936	0.78339	0.8451	1.21631	0.9207	1.64924	0.2888
0.37108	0.3217	0.80400	0.8632	1.23693	0.9069	1.66985	0.2348
0.39169	0.3502	0.82462	0.8800	1.25754	0.8914	1.69047	0.1737
0.41231	0.3790	0.84523	0.8956	1.27816	0.8744	1.71108	0.0998
0.43293	0.4080	0.86585	0.9098	1.29877	0.8557	1.73170	0.0000

TABLE X. The ^{17}F neutrino spectrum. The normalized ^{17}F neutrino energy spectrum $P(q)$ is given in intervals of 20.671 keV. The neutrino energy q is expressed in MeV and $P(q)$ is normalized per MeV.

q	$P(q)$	q	$P(q)$	q	$P(q)$	q	$P(q)$
0.02067	0.0014	0.45477	0.4375	0.88887	0.9223	1.32297	0.8323
0.04134	0.0056	0.47544	0.4666	0.90954	0.9337	1.34364	0.8103
0.06201	0.0123	0.49611	0.4957	0.93021	0.9436	1.36431	0.7866
0.08269	0.0214	0.51679	0.5245	0.95089	0.9521	1.38499	0.7614
0.10336	0.0328	0.53746	0.5531	0.97156	0.9590	1.40566	0.7347
0.12403	0.0463	0.55813	0.5813	0.99223	0.9645	1.42633	0.7064
0.14470	0.0618	0.57880	0.6091	1.01290	0.9683	1.44700	0.6765
0.16537	0.0791	0.59947	0.6363	1.03357	0.9706	1.46767	0.6451
0.18604	0.0980	0.62014	0.6629	1.05424	0.9713	1.48834	0.6121
0.20671	0.1185	0.64081	0.6888	1.07491	0.9704	1.50901	0.5776
0.22739	0.1404	0.66149	0.7140	1.09559	0.9679	1.52969	0.5414
0.24806	0.1635	0.68216	0.7383	1.11626	0.9638	1.55036	0.5035
0.26873	0.1878	0.70283	0.7617	1.13693	0.9580	1.57103	0.4638
0.28940	0.2131	0.72350	0.7841	1.15760	0.9506	1.59170	0.4221
0.31007	0.2393	0.74417	0.8056	1.17827	0.9415	1.61237	0.3782
0.33074	0.2662	0.76484	0.8259	1.19894	0.9308	1.63304	0.3317
0.35141	0.2938	0.78551	0.8451	1.21961	0.9184	1.65371	0.2818
0.37209	0.3219	0.80619	0.8631	1.24029	0.9044	1.67439	0.2275
0.39276	0.3504	0.82686	0.8799	1.26096	0.8888	1.69506	0.1663
0.41343	0.3793	0.84753	0.8954	1.28163	0.8716	1.71573	0.0927
0.43410	0.4083	0.86820	0.9095	1.30230	0.8527	1.73640	0.0000

been made in the input data for the solar models (in, e.g., the nuclear reaction rates, opacities, equation of state, and heavy element abundances) and in the sophistication and precision of the stellar evolution codes (e.g., the inclusion of diffusion). Throughout this whole period, the historically lowest rate corresponds, without diffusion, to 109 SNU (see the lowest point in Fig. 3, which occurs in 1969), which is more than 5σ larger than the combined experimental result from the GALLEX and SAGE experiments.

Detailed calculations and helioseismological measurements both show [41,42,52] that we must correct for the effects of diffusion the neutrino fluxes calculated prior to 1992 (cf. discussion in Sec. XII A). All of the standard model fluxes that my colleagues and I have calculated in the 30 years since 1968 lie in the range 120 SNU to 141 SNU, if the effects of diffusion are included.

The disagreement is robust between the predictions of standard solar models—supplemented by the assumption that nothing happens to the neutrinos after they are produced—and the results of gallium solar neutrino experiments.

How much could one conceivably reduce the calculated event rate in gallium neutrino experiments assuming standard neutrino physics, but nonstandard (or impossible) nuclear physics? The most efficient way to reduce artificially the calculated counting rate is by setting equal to zero the nuclear reaction rates that lead to higher-energy neutrinos in the solar model computations. This arbitrary procedure is physically impossible (the relevant nuclear fusion rates are measured in the laboratory to be comparable to rates that are not set equal to zero), but illustrates the extreme difficulty in reducing the calculated event rate to a rate close to what is measured in gallium solar neutrino experiments.

If we artificially eliminate all nuclear reactions that lead to ^{7}Be and ^{8}B neutrinos [i.e., assume that the cross section measured in laboratory experiments for the ^{3}He$(\alpha,\gamma)^4$He reaction is completely wrong and the reaction is forbidden for some unknown reason], then the rate calculated from standard solar models is $88.1^{+3.2}_{-2.4}$ SNU. This rate is about 2.5 σ larger than the measured rate in the GALLEX and SAGE experiments. Moreover, the same solar model predicts an event rate of 0.73 ± 0.01 SNU for the chlorine experiment, which is more than 8σ less than is observed.

One can consider solar models in which obviously incorrect assumptions about nuclear reactions are made for a number of different fusion reactions. If one assumes that not only does the ^{3}He$(\alpha,\gamma)^4$He reaction not occur, but also all four of the (p,γ) reactions in the CNO cycle (see footnote 2) do not occur, then one can calculate a solar model for which the capture rate is $79.5^{+2.3}_{-2.0}$ SNU. This capture rate corresponds to the minimum rate that is possible, ignoring all of the physics of solar models and making false assumptions about nuclear reactions, if one requires that the sun is currently producing thermal energy from nuclear fusion at the rate at which it is radiating energy via photons escaping from its surface. Even this most extreme model predicts an event rate that exceeds the current best-estimate rate, about 70.5 ± 7 SNU, observed by GALLEX [1] and SAGE [2]. The chlorine rate predicted by this most extreme model is 0.3 SNU, which is inconsistent with the observed rate of 2.54 ± 0.20 SNU [54].

C. What will GNO show?

Gallium solar neutrino experiments are the only established way of detecting the great majority of solar neutrinos,

the low-energy neutrinos from the fundamental pp reaction. Therefore, astronomical inferences and particle physics applications of solar neutrino studies rely strongly on the measured rates in gallium experiments. These inferences and applications will become more stringent as GNO reduces the statistical and the systematic uncertainties in the measured gallium rate.

The most exciting result that GNO might obtain is, in my opinion, to find a capture rate that is more than 3σ smaller than the minimum rate, $79.5^{+2.3}_{-2.0}$ SNU, calculated in Sec. XII B. This minimal rate is obtained by setting equal to zero five well-measured (and appreciable) nuclear reaction rates, and ignoring everything we know about the Sun except its total luminosity. If a number significantly less than 80 SNU were obtained, I believe that GNO by itself would establish that we require nonstandard neutrino physics in order to explain solar neutrino experiments. In fact, I think the same conclusion would be drawn if GNO ruled out by more than 3σ the unrealistically low rate of $88.9^{+3.2}_{-2.4}$ SNU obtained by arbitrarily excluding the nuclear reactions ^{3}He$(\alpha,\gamma)^7$Be that lead to ^{7}Be and ^{8}B neutrinos.

Will GNO find, after improvements in the statistics and in the systematic errors, that the best-estimate capture rate is significantly less than 88 SNU, or even less than 80 SNU? No one really knows, which is one of the reasons why the experiment is so important.

APPENDIX A

Table VII gives the normalized unmodified energy spectrum $P(q)$ for the pp neutrinos. The end point energy includes the average thermal energy of the fusing protons.

APPENDIX B

Table VIII gives the normalized unmodified energy spectrum $P(q)$ for the ^{13}N neutrinos. Table IX gives the normalized unmodified energy spectrum $P(q)$ for the ^{15}O neutrinos. Table X gives the normalized unmodified energy spectrum $P(q)$ for the ^{17}F neutrinos.

[1] W. Hampel *et al.*, Phys. Lett. B **388**, 384 (1996); P. Anselmann *et al.*, *ibid.* **357**, 237 (1995); **342**, 440 (1995); **327**, 377 (1994); **314**, 445 (1993); **285**, 276 (1992).

[2] J. N. Abdurashitov *et al.*, Phys. Lett. B **328**, 234 (1994); A. I. Abazov *et al.*, Phys. Rev. Lett. **67**, 3332 (1991); S. R. Elliott *et al.*, in *Electroweak Interactions and Unified Theories*, Proceedings of the XXXth Recontres de Moriond, Les Arcs, Savoie, France, edited by J. Trân Thanh Vân (Editions Frontieres, Singapore, 1995), p. 439.

[3] P. Anselmann *et al.*, Phys. Lett. B **342**, 440 (1995).

[4] W. Hampel *et al.*, Phys. Lett. B **388**, 384 (1996).

[5] M. Cribier *et al.*, Nucl. Instrum. Methods Phys. Res. A **265**, 574 (1988).

[6] V. Abdurashitov *et al.*, Phys. Rev. Lett. **77**, 4708 (1996).

[7] E. Bellotti *et al.*, ''Proposal for a Permanent Gallium Neutrino Observatory (GNO) at Laboratori Nazionali Del Gran Sasso,'' http://kosmopc.mpi-hd.mpg.de/gallex/gallex.html (1996).

[8] J. N. Bahcall, Phys. Rev. Lett. **23**, 251 (1969).

[9] N. Hata and W. Haxton, Phys. Lett. B **353**, 422 (1995).

[10] R. B. Firestone, in *Table of Isotopes*, 8th ed., edited by V. S. Shirley (Wiley, New York, 1996), p. 209.

[11] W. Hampel and L. P. Remsberg, Phys. Rev. C **31**, 666 (1985).

[12] W. Hampel and R. Scholtz, in *Proceedings of the 7th International Conference on Atomic Masses and Fundamental Constraints (AMCO-7)*, edited by E. Klepper (Darmstadt-Seeheim, 1984), p. 89.

[13] J. N. Bahcall and R. K. Ulrich, Rev. Mod. Phys. **60**, 297 (1988).

[14] J. N. Bahcall, *Neutrino Astrophysics* (Cambridge University Press, Cambridge, England, 1989).

[15] I. Žlimen, A. Ljubičić, and S. Kaučić, Phys. Rev. Lett. **67**, 560 (1991).

[16] D. E. DiGregorio *et al.*, Phys. Rev. C **47**, 2916 (1993).

[17] Y. S. Lee *et al.*, Phys. Rev. C **51**, 2770 (1995).

[18] G. Audi and A. H. Wapstra (private communication).

[19] J. N. Bahcall, Rev. Mod. Phys. **50**, 881 (1978).

[20] I. P. Grant, in *Atomic, Molecular, and Optical Physics Handbook* (American Institute of Physics, Woodbury, NY, 1996), Chap. 22, p. 258; F. A. Parpia, C. Froese Fischer, and I. P. Grant, Comput. Phys. Commun. **94**, 249 (1996); F. A. Parpia, M. Tong, and C. Froese Fischer, Phys. Rev. A **46**, 3717 (1992); also K. G. Dyall, I. P. Grant, C. T. Johnson, and F. A. Parpia, Comput. Phys. Commun. **55**, 425 (1989).

[21] W. R. Johnson and K. T. Cheng, in *Atomic Inner-Shell Physics*, edited by B. Crasemann, (Plenum, New York, 1985); Chap. 1, p. 3; W. R. Johnson and G. Soff, At. Data Nucl. Data Tables **33**, 405 (1985).

[22] Adaptation for Livermore National Laboratory of the multiconfiguration Dirac-Fock code described in I. P. Grant, B. J. McKenzie, P. H. Norrington, D. F. Mayers, and N. C. Pyper, Comput. Phys. Commun. **21**, 207 (1980).

[23] D. Krofcheck *et al.*, Phys. Rev. Lett. **55**, 1051 (1985).

[24] A. Sirlin, Rev. Mod. Phys. **50**, 573 (1978).

[25] W. Marciano (private communication).

[26] D. Krofcheck, Ph.D. thesis, Ohio State University, 1987.

[27] J. N. Bahcall, Phys. Rev. **129**, 2683 (1963).

[28] J. N. Bahcall, Nucl. Phys. **71**, 267 (1965).

[29] B. R. Holstein and S. B. Treiman, Phys. Rev. C **3**, 1921 (1971).

[30] J. N. Bahcall and B. Holstein, Phys. Rev. C **33**, 2121 (1986).

[31] V. A. Kuzmin, Ph.D. thesis, Lebedev Physics Institute, Moscow, 1967.

[32] R. S. Raghavan, Brookhaven National Laboratory Report No. 50879, 1978 Vol. 2.

[33] J. N. Bahcall, P. I. Krastev, and E. Lisi, Phys. Lett. B **348**, 121 (1995).

[34] W. Hampel (private communication).

[35] W. Heuer, Z. Phys. **194**, 224 (1966).

[36] K. Hikasa *et al.*, Phys. Rev. D **45**, S1 (1992).

[37] T. N. Taddeucci *et al.*, Nucl. Phys. **A469**, 125 (1987); K. Kubodera and S. Nozawa, Int. J. Mod. Phys. E **3**, 101 (1994); C. D. Goodman *et al.*, Phys. Rev. Lett. **44**, 1755 (1980).

[38] J. N. Bahcall, Phys. Rev. D **44**, 1644 (1991).

[39] See http://www.sns.ias.edu/~jnb, solar neutrino software and data.

[40] J. N. Bahcall, Phys. Rev. D **49**, 3923 (1994).

[41] J. N. Bahcall and M. P. Pinsonneault, Rev. Mod. Phys. **64**, 885 (1992).

[42] J. N. Bahcall and M. P. Pinsonneault, Rev. Mod. Phys. **67**, 781 (1995).

[43] J. N. Bahcall, E. Lisi, D. E. Alburger, L. De Braeckeleer, S. J. Freedman, and J. Napolitano, Phys. Rev. C **54**, 411 (1996).

[44] W. C. Haxton, Phys. Rev. C **38**, 2474 (1988).

[45] W. H. Press, S. A. Teukolsky, W. T. Vetterling, and B. P. Flannery, *Numerical Recipes in Fortran*, 2nd ed. (Cambridge University Press, Cambridge, England, 1992).

[46] J. N. Bahcall, W. A. Fowler, I. Iben, and R. L. Sears, Astrophys. J. **137**, 344 (1963).

[47] R. Davis, Jr., Phys. Rev. Lett. **12**, 303 (1964).

[48] J. N. Bahcall, Phys. Rev. Lett. **12**, 300 (1964).

[49] W. M. Good, W. E. Kunz, and C. D. Moak, Phys. Rev. **94**, 87 (1954).

[50] P. D. Parker, J. N. Bahcall, and W. A. Fowler, Astrophys. J. **139**, 602 (1964).

[51] J. N. Bahcall and R. Davis, Jr., in *Essays in Nuclear Astrophysics*, edited by C. A. Barnes, D. D. Clayton, and D. N. Schramm (Cambridge University Press, Cambridge, England, 1982), Chap. 12, p. 243. Also, reprinted as an Appendix to Ref. [14].

[52] J. N. Bahcall, M. H. Pinsonneault, S. Basu, and J. Christensen-Dalsgaard, Phys. Rev. Lett. **78**, 171 (1997).

[53] J. N. Bahcall, B. T. Cleveland, and R. Davis, Jr., Astrophys. J. **292**, 79 (1985).

[54] B. T. Cleveland, T. Daily, R. Davis, Jr., J. R. Distel, K. Lande, C. K. Lee, and P. S. Wildenhain, Astrophys. J. (in press); R. Davis, Jr., Prog. Part. Nucl. Phys. **32**, 13 (1994).

[55] Kamiokande Collaboration, Y. Fukuda *et al.*, Phys. Rev. Lett. **77**, 1683 (1996).

[56] J. N. Bahcall, B. T. Cleveland, R. Davis, Jr., and J. K. Rowley, Astron. J. Lett. **292**, 79 (1985); J. N. Bahcall, W. F. Huebner, S. H. Lubow, P. D. Parker, and R. K. Ulrich, Rev. Mod. Phys. **54**, 767 (1982); J. N. Bahcall, S. H. Lubow, W. F. Huebner, N. H. Magee, Jr., A. L. Merts, M. F. Argo, P. D. Parker, B. Rozsnyai, and R. K. Ulrich, Phys. Rev. Lett. **45**, 945 (1980); J. N. Bahcall and R. K. Ulrich, Astron. J. Lett. **160**, 57 (1970); J. N. Bahcall and R. K. Ulrich, Astrophys. J. **170**, 593 (1971); J. N. Bahcall, W. F. Heubner, N. H. McGee, A. L. Merts, and R. K. Ulrich, *ibid.* **184**, 1 (1973); J. N. Bahcall, N. A. Bahcall, and R. K. Ulrich, *ibid.* **156**, 559 (1969); J. N. Bahcall, N. A. Bahcall, and R. K. Ulrich, Astron. J. Lett. **2**, 91 (1968); J. N. Bahcall and G. Shaviv, Astrophys. J. **153**, 113 (1968); J. N. Bahcall, N. A. Bahcall, and G. Shaviv, Phys. Rev. Lett. **20**, 1209 (1968); J. N. Bahcall, Phys. Rev. Lett. **12**, 300 (1964).